GAW Report No. 243

Report of the Fifth Erythemal UV Radiometers Intercomparison

Buenos Aires, Argentina, 2018

WEATHER CLIMATE WATER

WORLD METEOROLOGICAL ORGANIZATION

GLOBAL ATMOSPHERE WATCH

GAW Report No. 243

Report of the Fifth Erythemal UV Radiometers Intercomparison

Buenos Aires, Argentina, 2018

Fernando Nollas[1], Eduardo Luccini[2,3], Gerardo Carbajal[1], Facundo Orte[5], Elian Wolfram[4,5], Gregor Hülsen[6], Julian Gröbner[6]

[1] Servicio Meteorológico Nacional, Argentina.
[2] CONICET - Centro de Excelencia en Productos y Procesos de Córdoba, Argentina.
[3] Facultad de Química e Ingeniería del Rosario, Pontificia Universidad Católica, Argentina.
[4] Consejo Nacional de Investigaciones Cientificas y Técnicas, CONICET, Argentina.
[5] Instituto de Investigaciones Científicas y Técnicas para la Defensa, CITEDEF, Argentina.
[6] Physikalisch-Meteorologisches Observatorium Davos/World Radiation Center, Switzerland.

WORLD METEOROLOGICAL ORGANIZATION

GLOBAL ATMOSPHERE WATCH

Chairperson, Publications Board
World Meteorological Organization (WMO)
7 bis, avenue de la Paix
P.O. Box 2300
CH-1211 Geneva 2, Switzerland

Tel.: +41 (0) 22 730 84 03
Fax: +41 (0) 22 730 80 40
E-mail: Publications@wmo.int

CONTENTS

EXECUTIVE SUMMARY

1. INTRODUCTION 1

2. BACKGROUND EXPERIENCES 3

3. RADIOMETERS 4
- 3.1 Reference radiometers 4
- 3.2 Sensors to calibrate 4

4. METHODOLOGY AND DATA ANALYSIS 6
- 4.1 Atmospheric conditions 6
- 4.2 Measurement protocol 7
- 4.3 Calibration procedure 9
- 4.4 Analysis of uncertainties 13

5. RESULTS 15

6. CONCLUSIONS 19

7. ACKNOWLEDGEMENTS 20

8. REFERENCES 21

ANNEX – Results 23

EXECUTIVE SUMMARY

This report presents the background information, procedures and results of the intercomparison of erythemal UV sensors carried out at the Central Observatory of Buenos Aires (OCBA) in 2018 against reference radiometers calibrated at the World Radiation Center (PMOD/WRC) in Davos during 2017. In this way, the data obtained at the measurement sites will be standardized and will be comparable locally and globally. Twenty sensors were calibrated, belonging to Argentine monitoring and research institutions. The associated relative uncertainty of each sensor was also estimated.

1. INTRODUCTION

Ultraviolet (UV) radiation sensors suffer the wear and tear caused by their outdoor exposition, under the solar radiation they measure, the inclemency of the weather, the effect of possible fluctuations of the electric current supply on the electronics of the instrument, etc. Therefore, it is crucial to perform regular comparisons of them against one or more standard sensors with traceability to the Physikalisch-Meteorologisches Observatorium Davos/World Radiation Center (PMOD/WRC), in a Radiometer Intercomparison (IC), so that the measurements obtained by these sensors at their respective sites are traceable and comparable, locally and globally.

The Servicio Meteorológico Nacional (SMN) has an erythemal UV solar radiation Monitoring Network with stations covering a wide range of the country's geography, some of them jointly installed with the Argentine Instituto de Investigaciones Científicas y Técnicas para la Defensa (CITEDEF).

The most complete calibration process for erythemal UV radiometers (also called UV-biometers) comprises of two stages: one for laboratory characterization and another for field calibration. The laboratory stage, using artificial UV radiation, consists in characterizing the instrument in all aspects: spectral response, cosine response, azimuthal dependence, linearity and estimation of their absolute calibration constant (under laboratory conditions). Complementarily, through the field calibration exposed to solar radiation, if a very reliable spectroradiometer is available the absolute calibration constant (under sun exposure conditions) is accurately established and, if the ozone layer can be measured with a precise instrument, the factors of conversion to erythemal irradiance for those conditions of solar zenith angle (SZA) and ozone column, making use of the spectral response measured in the laboratory. Finally, a reliable atmospheric UV radiative transfer model is used and the spectral response is determined in the laboratory to extend the conversion factors to erythemal irradiance, in a conversion matrix that covers the whole range of possible values of SZA and ozone vertical column under which each instrument could measure at their Station. Details can be found in Hülsen and Gröbner [1].

Since in our case we do not have the sophisticated instruments necessary to perform the laboratory characterization and the detailed field calibration, what is done in this case during the IC is the transference, in field conditions, of the absolute calibration of a fully calibrated UV radiometer to the other UV radiometers.

Although these campaigns are conveniently planned for dates close to the summer solstice, logistic reasons as well as extensive periods of cloudiness and rain prevented their quick development. In spite of this, 19 of the 20 radiometers were calibrated by the end of April 2018, and the only remaining sensor was calibrated finally during June 2018. Nevertheless, as a Regional Center (Region III) for the calibration of solar radiation sensors as designated by the World Meteorological Organization (WMO), it meant for the OCBA a significant pilot experience for future UV IC that allow Argentine institutions to regularly calibrate their instruments and project this type of event at regional level.

This report presents the background, procedures and results of the erythemal UV radiometers IC carried out at the Central Observatory of Buenos Aires (34.59ºS, 58.48ºW, 32m a.s.l.) in the whole period from 14 February to 5 June 2018, against two reference sensors fully calibrated during 2017 by PMOD/WRC in Davos.

---

2. BACKGROUND EXPERIENCES

The OCBA has been the headquarters of several previous ICs of erythemal UV sensors. The first of them was an itinerant IC deployed from October 1998 to April 1999, where UV biometers were calibrated "in situ" through a travelling UV reference biometer which took measurements for about 10 days simultaneously with each station's biometer, and included a thorough analysis of the uncertainties associated with their measurements [2].

Subsequently, in November 2006, through an IC, the sensors were recalibrated by Julian Gröbner using a Solar Light 501A reference sensor from the PMOD/WRC which had been calibrated three months earlier during the PMOD/WRC-COST726 action [3]. In this IC, the only clear day during the campaign was used to obtain the calibration factors. In 2010, he was the same PMOD/WRC researcher who again headed the UV sensor IC with the difference that many countries in the region participated in it. In this IC two standard sensors were used, one Solar Light 501A (SL) and the other Kipp & Zonen (K&Z). The local calibration procedure was described by Hülsen and Gröbner [1] who require to establish the spectral and angular response of each sensor. Due to the impossibility to completely characterize the sensors due to the lack of a characterization laboratory, it was recommended that nominal angular and spectral response functions for the sensors of the companies Solar Light and Yankee Environmental Systems (YES) should be used, which were obtained in the Davos laboratory based on their experience calibrating this type of sensors there.

The last IC was carried out in 2014 by SMN personnel at the OCBA against Solar Light 501A radiometer S/N 16723, which was calibrated a few months later by the PMOD/WRC in 2015.

3. RADIOMETERS

3.1 Reference radiometers

The radiometers chosen as references for the present IC were the SL S/N14078 belonging to the SMN and the YES S/N090703 belonging to CITEDEF, both fully calibrated in Davos during the "International UV Filter Radiometer Comparison 2017" [4].

SL 14078 sensor was also calibrated in the intercomparisons of 2010 (calibration factor 0.96) and 2014 (calibration factor 1.11). By 2017, their calibration factor is 1.086 with a relative uncertainty of 6.7% for small SZA.

On the other hand, YES090703 sensor obtained a calibration factor of 0.1305 W/m^2V in the 2017 Davos intercomparison, also with a relative uncertainty of 6.7% for small SZA.

3.2 Sensors to calibrate

Table 1 details the UV sensors that participated in the present IC and the station where they regularly measure. Together with the station’s UV radiometer at Buenos Aires there are other four UV sensors which have not a datalogger and they are stored as a replacement in case some other sensor has a fault. They were also calibrated despite the fact that some ones show performance problems such as non-stabilization of temperature or sensory surface deterioration caused by humidity that was not absorbed by the silica gel. Most of the SL sensors have been measuring since their installation at the Stations by years 1996-1999. The YES sensors located at Neuquén, Comodoro Rivadavia, Villa Martelli, Bariloche and Río Gallegos, and the two Kipp & Zonen of Pilar (Córdoba) and Tucumán, are part of SAVER-Net network that SMN and CITEDEF has deployed within the framework of the Project for Development of the Atmospheric Environmental Risk Management System in South America with the support of Japan International Cooperation Agency (JICA) and Japan Science and Technology (JST) (www.savernet-satreps.org).

SL 1870 and SL 2753 radiometers will be reinstalled in other places after the IC because there are YES radiometers belonging to the SAVER-NET project in the measurement sites where they were until now.

Table 1. Radiometers that participated in the IC and their measurement sites

ID INSTRUMENT	TYPE OF RADIOMETER	MEASUREMENT SITE	OBSERVATIONS
SL 14078	Solar Light 501	-	Reference
SL 1866	Solar Light 501	BUENOS AIRES	No Temperature Stabilisation
SL 1870	Solar Light 501	COMODORO RIV.	
SL 1871	Solar Light 501	BUENOS AIRES	No Temperature Stabilisation
SL 2711	Solar Light 501	BUENOS AIRES	Detector surface bad
SL 2747	Solar Light 501	BUENOS AIRES	Detector surface bad
SL 2748	Solar Light 501	MENDOZA	No Temperature Stabilisation
SL 2753	Solar Light 501	PILAR(CORDOBA)	Detector surface bad
SL 9002	Solar Light 501	USHUAIA	
SL 9004	Solar Light 501	BUENOS AIRES	No Temperature Stabilisation and detector surface bad
YES 090703	YES UVB-1	-	Reference
YES 60703	YES UVB-1	NEUQUÉN	
YES 130803	YES UVB-1	COMODORO RIV.	
YES 130804	YES UVB-1	VILLA MARTELLI	
YES 130805	YES UVB-1	BARILOCHE	
YES 130806	YES UVB-1	RIO GALLEG.	
YES 940602	YES UVB-1	LA QUIACA	
YES 970809	YES UVB-1	ROSARIO	
YES 970811	YES UVB-1	CÓRDOBA	
K&Z 170212	Kipp & Zonen UVS-E-T	PILAR(CORDOBA)	
K&Z 170213	Kipp & Zonen UVS-E-T	TUCUMÁN	
K&Z 120059	Kipp & Zonen UVS-E-T	SALTA	

4. METHODOLOGY AND DATA ANALYSIS

4.1 Atmospheric conditions

Figure 1 shows the behaviour of the ambient temperature and relative humidity (RH) during the period considered. These parameters were obtained in an hourly manner in the surface station that is inside the OCBA and it can be seen that since mid-April the RH is very high as a result of cloudiness and abundant rainfall.

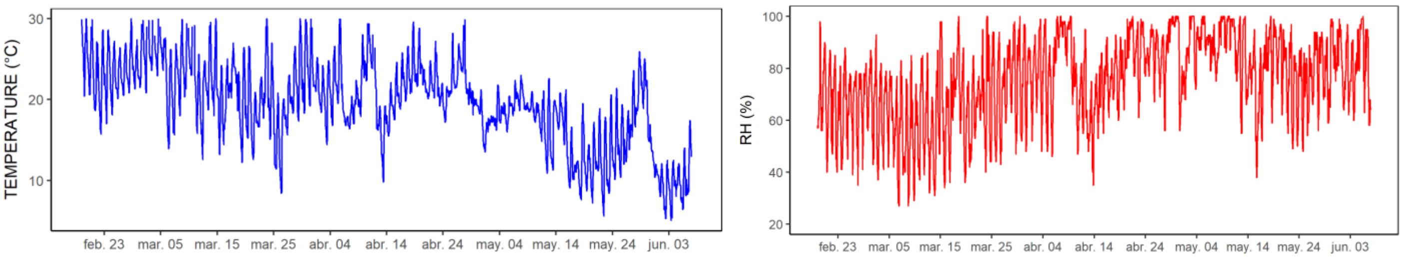

Figure 1. Ambient temperature and relative humidity measured in the OCBA during the calibration period.

On the other hand, the daily total ozone column is also measured in OCBA using a Dobson spectrophotometer (S/N # 70) which is, in turn, the regional standard assuring reliability in the values. Figure 2 illustrates the daily variability of ozone, a parameter that modifies surface UV radiation taking into account that the missing data in the measurement are due to the impossibility to measure during rainy days. It can be observed in the figure that during May, many values are missing and this is because that month there was abundant precipitation. Although this campaign was designed and planned to be carried out as closely as possible to the summer solstice, logistical and transport problems and mainly meteorological conditions forced us to extend it until June.

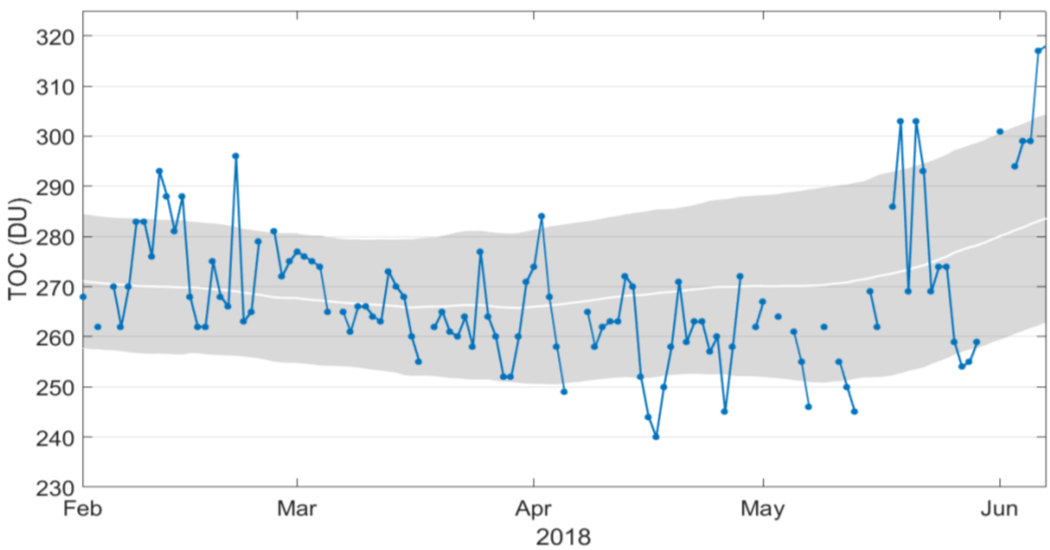

Figure 2. Daily total ozone column measured in the OCBA and expressed in Dobson Units (blue dot-line). Total ozone column climatology (1978-2013) (white line) and +/- 1 Standard Deviation (grey area) for Buenos Aires [5].

Figure 3 shows the data regarding the optical thickness of aerosols, a parameter that can affect the measurements of solar radiation on the surface. It can be seen that this parameter remained within normal values with respect to climatological values of aerosol loads, except for one day at the end of April and another at the end of May.

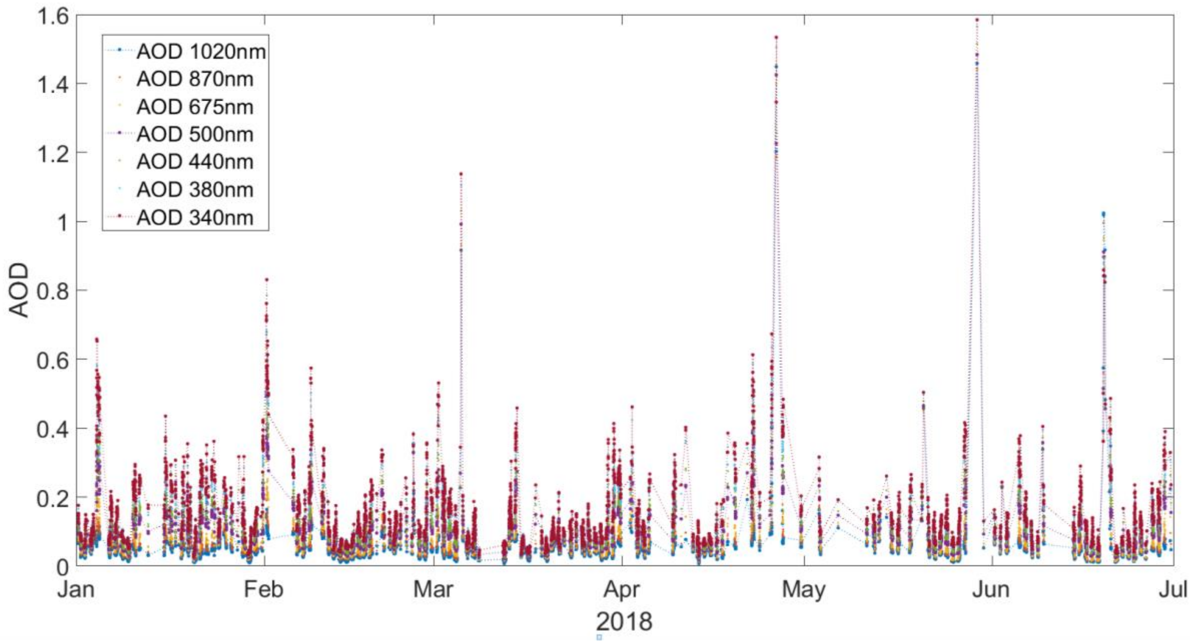

Figure 3. Optical thickness of aerosols measured in the city of Buenos Aires for the intercomparison period. Each colour corresponds to a determined wavelength of measurement.

The graph itself and the data shown in Figure 3 were reported on the website of the Aeronet network [6].

4.2 Measurement protocol

All the sensors were placed on a platform designed exclusively to carry out intercomparison of solar radiation sensors which is located on the roof of the Dobson box. Figure 4 illustrates the location of the sensors on the counter and it can be seen part of the trees surrounding the site. The effect of the interference produced by trees was quantified [2] and it was possible to verify in-situ that the shade produced by the vegetation was only projected on the sensors during the first part of the morning and the end of the day. In addition, due to the range of SZA that were considered for the calculations, and taking into account the fact that all the sensors measured on the same platform then the possible mitigating effects of the surrounding grove were not considered.

Figure 4. UV radiometers installed in the calibration platform in order to ensure that the irradiance received is the same.

Due to the complex logistics within the country, not all radiometers could arrive at the OCBA at the end of February as planned. Table 2 shows the period during which each of the radiometers was measuring together with the reference UV radiometers. As can be seen in Table 2, by April 23, 19 of the 20 radiometers had already been contrasted against the reference radiometers. Due to shipping problems, the K&Z 120059 sensor arrived at the OCBA in mid-April and was installed on April 25, but the weather conditions prevented it from being calibrated, so it had to measure until the beginning of June, when there were clear days.

Table 2. Period along the IC during which each of the UV radiometers was measuring together with the reference UV radiometers.

ID RADIOMETER	*MEASUREMENT PERIOD*
SL 1866	28-03 to 15-04
SL 1870	07-03 to 27-03
SL 1871	21-02 to 05-03
SL 2711	28-03 to 15-04
SL 2747	21-02 to 01-03
SL 2748	20-02 to 05-03
SL 2753	13-03 to 24-03
SL 9002	09-03 to 27-03
SL 9004	28-03 to 15-04
YES 60703	14-04 to 23-04
YES 130803	06-03 to 27-03

YES 130804	28-03 to 16-04
YES 130805	12-03 to 27-03
YES 130806	28-03 to 16-04
YES 940602	28-02 to 15-03
YES 970809	19-02 to 05-03
YES 970811	15-03 to 27-03
K&Z 170212	13-03 to 27-03
K&Z 170213	09-03 to 27-03
K&Z 120059	25-04 to 05-06

The sensors to be calibrated were installed as they arrived at the OCBA from their different measurement destinations, with an average time of intercomparison against the reference instruments of approximately 15 days. After this time, when at least 3 days were completely clear, the sensors were uninstalled and sent to the measurement site where they normally perform the measurements.

All radiometers received maintenance, which consisted in daily cleaning the external dome using laboratory-grade isopropyl alcohol and verifying the state of the silica gel for moisture absorption.

Once installed on the platform, the digital SL sensors were connected to their respective acquisition unit in which a scale factor of 10 was applied to increase the resolution of the stored values as integrated MED doses over 1 minute. On the other hand, all YES and K&Z radiometers were connected to a Campbell CR1000 datalogger which was configured to obtain one voltage output per minute, which represents the average of instantaneous measurements every 10 seconds. All values were accompanied by their respective measurement time which was expressed in UTC time. In the case of the SL sensors, the raw values obtained by them were transformed to irradiance through the multiplication of the 0.35 factor.

SL radiometers have the particularity that the acquisition unit stores the minute MED dose values and also the internal temperature of the sensor, which makes it possible to verify whether it is thermally stabilized. This allowed us identifying sensors that did not regulate the temperature and therefore a correction established in the manual of this type of instruments had to be added. On the other hand, the YES and K&Z sensors also allow us to obtain the value of the resistance associated with temperature control, but due to space constrains in the datalogger only the values of solar radiation of the majority of them were registered without taking into account the measurement of temperature. The sensors connected to the Campbell datalogger in which the temperature stabilization was confirmed were the reference YES090703, both K&Z, YES130806 and YES130840, confirming that they all regulated.

4.3 Calibration procedure

Before initiating the UV IC, only the reference sensors were installed to evaluate and compare the values found by both and, in turn, they were contrasted against those obtained using the TUV (Tropospheric Ultraviolet and Visible) radiative transfer clear sky model. To perform this comparison, the UV Index (UVI) measured by each of the sensors was calculated, which represents a measure of the intensity of UV radiation and its ability to cause injury to humans. The UVI is obtained mathematically by multiplying the erythemal irradiance in Wm-2 by 40 and was adopted by the World Health Organization (WHO) and WMO as the approved indicator to inform the population about the risk before exposure to solar radiation. More information on this parameter and a guide for its understanding can be found in reference [7].

It was found that the UVI values measured by YES090703 were slightly higher than those measured by SL14078 and those estimated by the TUV model, the values of the latter being located between the measurements of the sensors. This can be seen in Figure 5 where the UVI values of the data available for both sensors are shown and estimated by the model for the 14th and 15th of February. Using the data measured by both standards it was observed that, for SZA less than 70° and days of clear sky, the relative difference between both for days of clear sky did not exceed the value of 7% and taking into account the experimental error of both sensors it was possible to assure that the values were similar and could thus be taken as references for the UV IC. In the same way, it was found that, for days with variable cloudiness, the relative difference in the measurements represented variations of different intensity, so the decision was made to consider moments of clear sky for the calculations. It is for this reason that weather conditions were a limiting parameter during the present IC and therefore its extension.

Once the experimental equality of the values found by both radiometers was determined, it was decided to use the SL14078 as a secondary standard for the UV IC because its angular response resembles the ideal one more than the YES 090703 sensor and also its spectral response is more similar to the of the erythema proposed by McKinlay and Diffey [8]. Although both sensors have a complete characterization in the Davos laboratory (Section 3.1) that makes it possible to correct these differences, another reason why the SL14078 was chosen was because it had previous calibrations without showing a significant difference about its stability. Likewise, due to a problem in its acquisition unit, the SL14078 sensor had to be replaced by the YES090703 as a secondary reference on March 19.

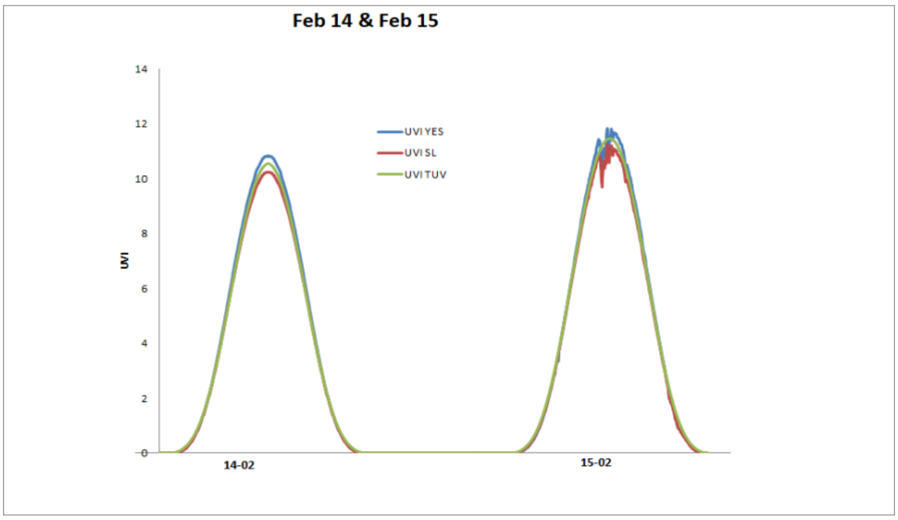

Figure 5. Qualitative comparison of the values measured by both reference sensors and the TUV model for February 14 and 15.

The calibration procedure to be used was the one described by Hülsen and Gröbner [1] where it is stated that erythemal irradiance can be obtained from equation 1.

$$E_{CIE} = (U - U_{offset}) C f_n(SZA, TO_3) Coscor, \tag{1}$$

where U represents the raw output signal, U_{offset} the night signal and C is the absolute calibration constant. The conversion function (or transfer matrix) f_n is normalized to a zenith angle (SZA) of 40° as well as ozone column (TO3) of 300 DU and is obtained through radiative transfer models using the spectral response of each sensor measured in the laboratory. The remaining Coscor parameter is also obtained from laboratory measurements and represents the correction of the intrinsic cosine error of each instrument.

As explained in Section 3.1, these parameters are completely known for the standard sensors since both were calibrated by the PMOD/WRC in the laboratory and field or outdoor. Also the only radiometers calibrated in this campaign for which its matrix were know the K&Z 170212 and K&Z 170213, which was obtained at the factory. Since the angular and spectral responses of the rest of the instruments to be calibrated during this UV IC are not known, it was decided to follow the guidelines used by Julian Gröbner in the UV IC that he carried out previously in 2010. On that occasion, nominal spectral and angular angles response functions were used for the sensors obtaining the transfer matrices and cosine corrections shown in Tables 3 to 6. Although these corrections are not properly measured for each radiometer, they were obtained as an average of characterizations made in Davos for each type of manufacturer company. On the other hand, Table 7 shows the average cosine correction for the K&Z radiometers [Personal communication with Gregor Hülsen] obtained in the Davos laboratory as an average for this type of sensors.

Table 3. Conversion function according to the SZA and the ozone column in DU for the SL 501 radiometers normalized to SZA = 40 ° and TO3 = 300 DU.

	200	**220**	**240**	**260**	**280**	**300**	**320**	**340**	**360**	**380**	**400**
0	1.093	1.072	1.055	1.041	1.029	1.019	1.012	1.006	0.998	0.998	0.996
5	1.092	1.072	1.054	1.04	1.028	1.019	1.011	1.005	0.998	0.998	0.996
10	1.09	1.069	1.052	1.038	1.027	1.017	1.01	1.005	0.998	0.998	0.996
15	1.085	1.065	1.049	1.035	1.024	1.015	1.008	1.003	0.997	0.997	0.996
20	1.079	1.06	1.044	1.031	1.02	1.012	1.006	1.002	0.997	0.997	0.996
25	1.072	1.053	1.038	1.026	1.016	1.009	1.004	1	0.997	0.997	0.997
30	1.063	1.045	1.031	1.02	1.012	1.005	1.001	0.999	0.998	0.998	0.999
35	1.052	1.036	1.024	1.014	1.007	1.002	0.999	0.998	1	1	1.002
40	1.041	1.027	1.016	1.008	1.003	1	0.999	0.999	1.004	1.004	1.008
45	1.03	1.018	1.009	1.004	1.001	1	1.001	1.003	1.012	1.012	1.018
50	1.019	1.01	1.009	1.001	1.001	1.003	1.007	1.012	1.025	1.025	1.034
55	1.01	1.004	1.002	1.003	1.006	1.012	1.019	1.027	1.047	1.047	1.059
60	1.005	1.004	1.007	1.012	1.02	1.029	1.04	1.053	1.081	1.081	1.096
65	1.008	1.013	1.021	1.032	1.045	1.06	1.077	1.094	1.133	1.133	1.154
70	1.023	1.036	1.052	1.071	1.091	1.113	1.137	1.161	1.213	1.213	1.241
75	1.061	1.084	1.11	1.139	1.169	1.2	1.233	1.267	1.337	1.337	1.373
80	1.138	1.175	1.214	1.225	1.298	1.343	1.388	1.434	1.527	1.527	1.575
85	1.278	1.332	1.387	1.444	1.502	1.561	1.62	1.68	1.8	1.8	1.86
90	1.379	1.432	1.49	1.549	1.609	1.67	1.732	1.795	1.921	1.921	1.984

Table 4. Average Clear sky Cosine Correction function Coscor for YES radiometer UVB-1.

0	5	10	15	20	25	30	35	40	45	50	55	60	65	70	75	80	85	90
1.07	1.07	1.08	1.08	1.08	1.09	1.1	1.11	1.12	1.13	1.15	1.16	1.18	1.2	1.21	1.2	1.19	1.17	1.17

Table 5. Average Clear sky Cosine Correction function Coscor for SL radiometer 501.

0	5	10	15	20	25	30	35	40	45	50	55	60	65	70	75	80	85	90
1.02	1.02	1.03	1.02	1.02	1.02	1.02	1.02	1.02	1.02	1.03	1.03	1.04	1.05	1.07	1.07	1.07	1.06	1.05

Table 6. Conversion function according to the SZA and the ozone column in DU for YES UVB-1 radiometers normalized to SZA = 40 ° and TO3 = 300 DU.

	200	220	240	260	280	300	320	340	360	380	400
0	1.249	1.202	1.162	1.128	1.099	1.074	1.053	1.034	1.018	1.005	0.993
5	1.247	1.2	1.16	1.127	1.098	1.073	1.052	1.033	1.017	1.004	0.992
10	1.241	1.195	1.155	1.122	1.093	1.069	1.048	1.03	1.014	1.001	0.99
15	1.231	1.185	1.147	1.114	1.086	1.062	1.042	1.025	1.01	0.997	0.986
20	1.217	1.173	1.135	1.103	1.077	1.054	1.034	1.017	1.003	0.991	0.981
25	1.2	1.157	1.121	1.09	1.064	1.042	1.024	1.008	0.995	0.984	0.975
30	1.179	1.137	1.103	1.074	1.05	1.03	1.012	0.998	0.986	0.976	0.968
35	1.154	1.115	1.083	1.056	1.034	1.015	1	0.987	0.977	0.968	0.962
40	1.127	1.091	1.061	1.036	1.016	1	0.987	0.976	0.967	0.961	0.956
45	1.097	1.064	1.038	1.016	0.999	0.985	0.974	0.966	0.959	0.955	0.952
50	1.066	1.037	1.014	0.996	0.982	0.971	0.963	0.958	0.954	0.953	0.952
55	1.035	1.01	0.992	0.978	0.968	0.961	0.957	0.954	0.954	0.956	0.958
60	1.005	0.987	0.974	0.965	0.959	0.957	0.957	0.959	0.963	0.968	0.975
65	0.981	0.969	0.963	0.96	0.96	0.963	0.969	0.976	0.985	0.995	1.007
70	0.967	0.964	0.965	0.97	0.977	0.988	1	1.014	1.03	1.047	1.065
75	1.061	1.084	1.11	1.139	1.169	1.2	1.233	1.267	1.302	1.337	1.373
80	1.138	1.175	1.214	1.255	1.298	1.343	1.388	1.434	1.48	1.527	1.575
85	1.278	1.332	1.387	1.444	1.502	1.561	1.62	1.68	1.74	1.8	1.86
90	1.379	1.434	1.49	1.549	1.609	1.67	1.732	1.795	1.858	1.921	1.984

Table 7. Cosine correction according to the SZA for the K&Z sensors

0	5	10	15	20	25	30	35	40	45	50	55	60	65	70	75	80	85	90
1.001	1	0.998	0.997	0.997	0.997	0.997	0.997	0.997	0.997	0.998	0.997	0.998	0.998	0.998	1.003	1.005	1.002	1.001

In days with a completely covered sky, it is considered that radiation reaches the surface in isotropic form, so in these cases we speak of a diffuse correction factor where the Coscor takes a constant value that is equal to 1.05 for the SL sensors, 1.17 for the YES and 1.001 for the K&Z sensors.

When establishing the relation between the values measured by the sensors to be calibrated (test) against those obtained by the standards, it was found that the discretization of the parameters at a step of 5° of SZA generated a substantial relative difference that increased as

the SZA grew. For this reason, we decided to perform a polynomial interpolation adjustment for each cosine conversion and correction matrix, both in standard sensors and in test sensors, which considered the 0-90° angles in order to establish a continuous behaviour of them.
For the calculations, parameters of eq.1 were used in order to correct the values obtained by the standard sensors to work them in $W.m^{-2}$. Likewise, for the sensors to be calibrated, the conversion and Coscor matrix corresponding to each manufacturer brand was used in order to obtain their absolute calibration constant (C). It is necessary to clarify that, for the final calculation of C, SZA <50 ° was considered except for the K&Z S / N 120059 sensor for which SZA less than 65 ° were used because data used for this sensor were for June SZA less than 50 ° were scarce for this sensor.

In the case of SL radiometers which do not stabilize temperature, the option available to the collector of the data was used to perform the theoretical automatic correction as explained in the manual of this radiometer mark. When consulting the manufacturing company for the validity of the correction, it assured that it is applicable between temperatures of 0°C and 50°C.

4.4 Analysis of uncertainties

For the analysis of uncertainties, the work of Cede et al. [2] was used as a reference and the following sources of uncertainty were considered:

- Uncertainty in standard instruments ($\sigma_{patrón}$)
- Statistical dispersion of the values obtained from C (σ_{disp})
- Errors in the nominal response functions used for the sensors (σ_{espec} and σ_{ang})
- Uncertainty in the output signal of the sensors (σ_{raw})

In their work, Cede et al. [2] analysed the multiple associated uncertainties and established their variation with respect to the zenith angle for the YES and SL radiometers that were in the UV network at that time. The resulting uncertainty obtained in that work taking into account the contributions of the angular and spectral response as well as the uncertainty in the output signal of the sensors is shown in Table 8.

Table 8. Relative uncertainty resulting from the combination of uncertainties in the angular and spectral responses as well as in the output signal from the sensors for the different zenith angles. Cede et al. (2000).

	SZA					
Uncertainties (%)	<30°	40°	50°	60°	70°	80°
Combination σ_{espect} , σ_{ang} ,σ_{raw}	6.0	6.1	6.5	7.6	10.6	18.7

For the present report, the results from Table 8 were used and the results obtained were added from the dispersion of the data and from the uncertainty inherent in the calibration of the reference obtained in Davos, which is 6.7% for both. Likewise, for the K&Z sensors a 3% relative uncertainty of the cosine correction was used, since this value represents the expected maximum uncertainty for this parameter according to the differences found by Hülsen and

Gröbner [4] while, for the matrix obtained in factory, an uncertainty of 3% was associated [personal communication with the manufacturing company]. There is no variation of the uncertainty with SZA for the K&Z, so the value found based on the values previously entered will be representative for the entire angular range of 0°-90°.

It should be pointed out that the uncertainty due to statistical dispersion was obtained from considering a normal distribution with a confidence interval of 95%.

For the calculation of the final relative uncertainty it was assumed that the independent uncertainties had zero covariance and equation 2 was used.

$$Relative uncertainty = \sqrt{\sigma_{patron}^2 + \sigma_{disp}^2 + \sigma_{espect}^2 + \sigma_{ang}^2 + \sigma_{raw}^2} \quad (2)$$

Since we do not have an average nominal matrix for the K&Z brand sensors, the uncertainty in the calibration increases significantly as quantified by Hülsen and Gröbner [4]. The authors found differences of up to 20% when not considering the transfer matrix and this was the base value associated with this magnitude for the K&Z 120059 sensor in the present work.

5. RESULTS

Table 9 lists the instruments, the absolute calibration factors found for each of them, measurement station, and a comparison with the last factor that has been recorded. The sensors called "back up" made measurements in different places but were replaced by new sensors, thus remaining saved for cases of malfunction in order not to lose data.

Table 9 shows different aspects to be analysed, one of the most striking being the fact that both the SL 1870 and the YES 940602 radiometers show the minimum difference in their calibration factor respect their factor since 2010. It is important to mention that SL 1870 radiometer always made measurements in the city of Comodoro Rivadavia, site with weather conditions are typically characterized by low humidity and temperatures that hardly exceed a 30°C. It should be noted that these same characteristics are observed in La Quiaca, the station where the YES940602 is located.

On the other hand, it is observed that the sensor SL 2748 has been the most degraded of all showing a variation of 42% with respect to its last calibration. This result shows that for future work in which the data is used where this sensor measured should be paid close attention and should be treated with care taking into account all possible corrections to be applied.

Another result to be analysed separately is that obtained from the radiometer K&Z 120059, which was the last to arrive in Buenos Aires for calibration. This radiometer could be contrasted the first days of June due to the rains and constant cloudiness in the city during May. The calibration constant for this radiometer, as explained above, was obtained using values with SZA less than 65° with a minimum of 56.6° so we would expect a difference with respect to whether smaller SZA had participated in the calculations.

It is observed that of the 9 SL radiometers, 4 of them do not stabilize temperature so, in case of being used, the correction provided by the factory must be taken into account. It was also possible to visually verify that the detector’s surface is slightly deteriorated in 3 of the 9 sensors, possibly due to humidity that has entered inside them by a saturated silica gel.

The SL 2711 sensor shows great variation with respect to its calibration in 2014, so its calibration history was revised, finding a great variability in its calibration constant over the years. The calibration factors of this sensor, obtained in 2006, 2010 and 2014 were 1.53, 1.09 and 1.14 respectively. The little stability of the sensor is evident so frequent re-calibration is highly recommended.

Table 9. Absolute calibration constants obtained for each one of the participating sensors of the UV 2018 IC, the station where they regularly measure and comparison with the last previous factor obtained.

ID RADIOMETER	MEASUREMENT SITE	CALIBRATION FACTOR 2018	PREVIOUS CALIBRATION FACTOR	YEAR OF PREVIOUS INTERCOMPARISON	CHANGE RATIO (%)	UNITS	COMENTS
SL 1866	BACKUP	1.17	1.30	2006	-10	-	No Temperature Stabilisation
SL 1870	MENDOZA	1.05	1.05	2010	0	-	
SL 1871	BACKUP	0.97	1.05	2014	-8	-	No Temperature Stabilisation
SL 2711	BACKUP	1.58	1.14	2014	39	-	Detector surface bad
SL 2747	BS AS	1.34	1.32	2014	2	-	Detector surface bad
SL 2748	BACKUP	1.76	1.24	2010	42	-	No Temperature Stabilisation
SL 2753	BACKUP	1.15	1.07	2010	7	-	Detector surface bad
SL 9002	USHUAIA	0.78	0.99	2010	-21	-	
SL 9004	BACKUP	0.92	1.08	2006	-15	-	No Temperature Stabilisation and detector surface bad
YES 60703	NEUQUEN	0.13	0.145	Factory	-10	(W/m2)/V	
YES 130803	COMODORO RIV.	0.12	0.132	Factory	-9	(W/m2)/V	
YES 130804	VILLA MART.	0.13	0.132	Factory	-1	(W/m2)/V	
YES 130805	BARILOCHE	0.12	0.132	Factory	-9	(W/m2)/V	
YES 130806	RIO GALLEG.	0.12	0.130	Factory	-7	(W/m2)/V	
YES 940602	LA QUIACA	0.12	0.12	2010	0	(W/m2)/V	
YES 970809	BACK UP	0.15	0.14	2010	10	(W/m2)/V	
YES 970811	CORDOBA	0.13	0.141	Factory	-8	(W/m2)/V	
K&Z 170212	PILAR	0.17	0.198	Factory	-14	(W/m2)/V	
K&Z 170213	TUCUMAN	0.18	0.203	Factory	-11	(W/m2)/V	
K&Z 120059	SALTA	0.15	0.189	2012	-21	(W/m2)/V	

Table 10 shows the number of measurements per sensor within the considered SZA range used to obtain the calibration factor, as well as their standard deviation. These were the used values to obtain the statistical dispersion term in the relative uncertainty of the sensors.

In Table 10 it can be observed that, in general, the quantity of values used to obtain the absolute constant is adequate for a statistical analysis. In addition, due to problems in acquiring data from YES130806 and SL2711sensors, only one day was useful for their analysis, limiting so the amount of data. Nevertheless, its calibration was considered adequate given the observed low dispersion with respect to the average.

Table 10. Amount of data used to calculate the absolute calibration constant and standard deviation.

ID Radiometer	*Stand. Desv.*	*Number of Measures*
SL 1866	0.01	406
SL 1870	0.01	1735
SL 1871	0.01	2281
SL 2711	0.02	301
SL 2747	0.02	1143
SL 2748	0.01	1143
SL 2753	0.01	1195
SL 9002	0.02	1608
SL 9004	0.01	406
YES 60703	0.001 $Wm^{-2}V^{-1}$	406
YES 130803	0.003 $Wm^{-2}V^{-1}$	1289
YES 130804	0.001 $Wm^{-2}V^{-1}$	663
YES 130805	0.002 $Wm^{-2}V^{-1}$	1955
YES 130806	0.001 $Wm^{-2}V^{-1}$	298
YES 940602	0.001 $Wm^{-2}V^{-1}$	2006
YES 970809	0.002 $Wm^{-2}V^{-1}$	1726
YES 970811	0.001 $Wm^{-2}V^{-1}$	1289
K&Z 170212	0.002 $Wm^{-2}V^{-1}$	942
K&Z 170213	0.001 $Wm^{-2}V^{-1}$	1182
K&Z 120059	0.005 $Wm^{-2}V^{-1}$	786

Table 11 contains the associated uncertainties based on the SZA, obtaining similar values for the SL and YES sensors but differentiating the K&Z. The latter is due to the fact that, for the two K&Z sensors whose matrix are known, the associated uncertainty is lower, while for the K&Z120059 radiometer a value of 22.2% is reached due to the unknown of their spectral response, as explained in Section 4.4.

Once the absolute calibration factor was obtained for each of the sensors, Eq. 1 with their respective corrections to each one of them was applied and the graphs of results are shown in the Annex where it can be seen in the same graph the UVI values measured by the reference standard sensor and the sensor calibrated against it. In the same figure the test/ref relation in function of the SZA is also shown where "test" is associated with the radiometer to be calibrated while "ref" represents the reference standard. Finally, the graph also shows the relative frequency of occurrence of each value obtained from that relationship. The graphs show that all the sensors measure adequately and the possible diurnal differences with respect to the reference are due to the fact that the assumed angular and spectral responses of the radiometers are not adequate for these radiometers. Due to a change in the configuration of the datalogger is that on April 13 there was no data available and therefore some sensors only show the UV index for April 14 and 15.

Table 11. Relative uncertainty of each sensor as a function of the zenith angle

Uncertainty (%)	<30°	40°	50°	60°	70°	80°
SL 1866	9.2	9.3	9.6	10.4	12.7	20.0
SL 1870	9.2	9.3	9.5	10.3	12.7	20.0
SL 1871	9.4	9.4	9.7	10.5	12.8	20.0
SL 2711	9.2	9.3	9.6	10.3	12.7	20.0
SL 2747	9.6	9.7	9.9	10.7	13.0	20.1
SL 2748	9.1	9.2	9.5	10.3	12.6	19.9
SL 2753	9.3	9.3	9.6	10.4	12.7	20.0
SL 9002	10.0	10.1	10.3	11.0	13.3	20.3
SL 9004	9.3	9.4	9.6	10.4	12.8	20.0
YES 60703	9.1	9.2	9.5	10.3	12.7	19.9
YES 130803	10.3	10.3	10.6	11.3	13.5	20.5
YES 130804	9.2	9.2	9.5	10.3	12.7	19.9
YES 130805	9.6	9.7	10.0	10.7	13.0	20.2
YES 130806	9.1	9.2	9.5	10.3	12.6	19.9
YES 940602	9.1	9.1	9.4	10.2	12.6	19.9
YES 970809	9.5	9.5	9.8	10.6	12.9	20.1
YES 970811	9.0	9.1	9.4	10.2	12.6	19.9
K&Z 170212	8.3	8.3	8.3	8.3	8.3	8.3
K&Z 170213	8.0	8.0	8.0	8.0	8.0	8.0
K&Z 120059	22.2	22.2	22.2	22.2	22.2	22.2

6. CONCLUSIONS

During the firsts months of 2018 the UV radiometer's intercomparison was carried out at the Central Observatory of Buenos Aires, in which 20 sensors belonging to different Argentine operational and research institutions participated. During the intercomparison, Solar Light and a Yankee Environmental Systems radiometers with S/N 14078 and 090703 respectively were used as standards, both calibrated in Davos by the PMOD/WRC in 2017 and the calibration factor and its associated relative uncertainty of each of the participant sensors were obtained. For the calibration of the instruments, a transfer matrix and a cosine correction vector obtained through the use of average nominal spectral and angular responses were used for the Solar Light and YES companies provided by PMOD/WRC personnel in the last intercomparison of 2010. The K&Z sensors had factory-obtained matrices and a cosine correction vector obtained as an average for this brand of sensors was also used. The measurements of the K&Z 120059 radiometer were only corrected by the cosine correction vector so they were associated with a much higher uncertainty than for the rest.

It was observed that while some of the SL sensors showed deterioration in the detector surface, others did not stabilize temperature. This may be due to weather conditions and maintenance, so a change of the silica gel is recommended in adequate atmospheric conditions. Results in the calibration constants were compared to the ones obtained during the intercomparison carried out in 2010 and 2014, finding differences that reach 42% with respect to the last calibration, although it is worth mentioning that for several of the sensors, the last intercomparison was in 2010. On the other hand, it is observed that the instruments marking a smaller difference with respect to their previous calibration in 2010 were found in stations characterized by low relative humidity throughout the year as well as temperatures that rarely exceed 30 °C.

It was found the ratio of the corrected values obtained by almost all the sensors, once calibrated with respect to the values measured by the reference radiometer, moves away from the value 1 as the zenith angle increases. This could be associated to the fact that the angular and spectral responses of the instruments were not obtained for each radiometer but that nominal responses were used for each type of radiometer. For the K&Z sensors it is observed that the S/N 170213 and S/N 170212 radiometers do not depart so much from the unit value because their factory correction matrix is known and the cosine correction value does not vary much with the SZA. Finally, the S/N 120059 radiometer shows a behaviour very different from the rest and this could be due to the fact that no type of correction matrix was used.

Because of its traceability to the WRC, the new calibration factor will allow comparable measurements between radiometers thus assuring reliability in the data obtained.

7. ACKNOWLEDGEMENTS

We would like to thank CITEDEF for providing us with one of the calibrating instruments without which the intercomparison could not have been carried out and CITEDEF staff, Raúl D'Elia and Claudio Libertelli for their continuous contributions.

It is worth highlighting the efforts made by German Pérez Fogwill, Francisco Sosa and Ricardo Sánchez who installed, programmed and maintained the calibrated sensors. Without them, the intercomparison could not have taken place either.

We would also like to thank Sebastian Papandrea for his work in the logistics transport of all the sensors to be calibrated and to all the observers and personnel in charge of the operation and maintenance of the sensors in the measurement sites.

Professional staff from the different institutions that participated in the Intercomparison.

____

8. REFERENCES

[1] Hülsen G., J. Gröbner, 2007: Characterization and calibration of ultraviolet broadband radiometers measuring erythemally weighted irradiance. *Applied Optics*, 46, 5877-5886, 2007.

[2] Cede, A., E. Luccini, R.D. Piacentini, L. Nunez and M. Blumthaler, 2002a: Calibration and Uncertainty Estimation of Erythemal Radiometers in the Argentine Ultraviolet Network. *Applied Optics*, 41(30), 6341–6350.

[3] G. Hülsen, J. Gröbner, A. Bais, M. Blumthaler, P. Disterhoft, B. Johnsen, K.O. Lantz, C. Meleti, J. Schreder, J.M. Vilaplana Guerrero, L. Ylianttila, 2008: Intercomparison of erythemal broadband radiometers calibrated by seven UV calibration facilities in Europe and the USA. *Atmospheric Chemistry and Physics*, 8 (16), 4865–4875.

[4] World Meteorological Organization, 2018: Report of the Second International UV Filter Radiometer Calibration Campaign UVC-II. Davos, Switzerland, 25 May–5 October 2017. GAW Report No. 240.

[5] Van der A, R. J., M.A.F. Allaart and H.J. Eskes, 2015: Extended and refined multi sensor reanalysis of total ozone for the period 1970–2012. *Atmospheric Measurement Techniques*, 8, 3021-3035, https://doi.org/10.5194/amt-8-3021-2015, 2015.

[6] https://aeronet.gsfc.nasa.gov/

[7] http://www.who.int/uv/publications/globalindex/es/

[8] McKinlay A.F., B.L. Diffey, 1987: A reference action spectrum for ultraviolet induced erythema in human skin. En: W.R. Passchier, B.F.M. Bosjanokovic (Eds), Human Exposure to Ultraviolet Radiation: Risks and Regulations. *Elsevier*, Amsterdam. 83-7.

ANNEX

RESULTS OBTAINED FOR SENSOR SL1866

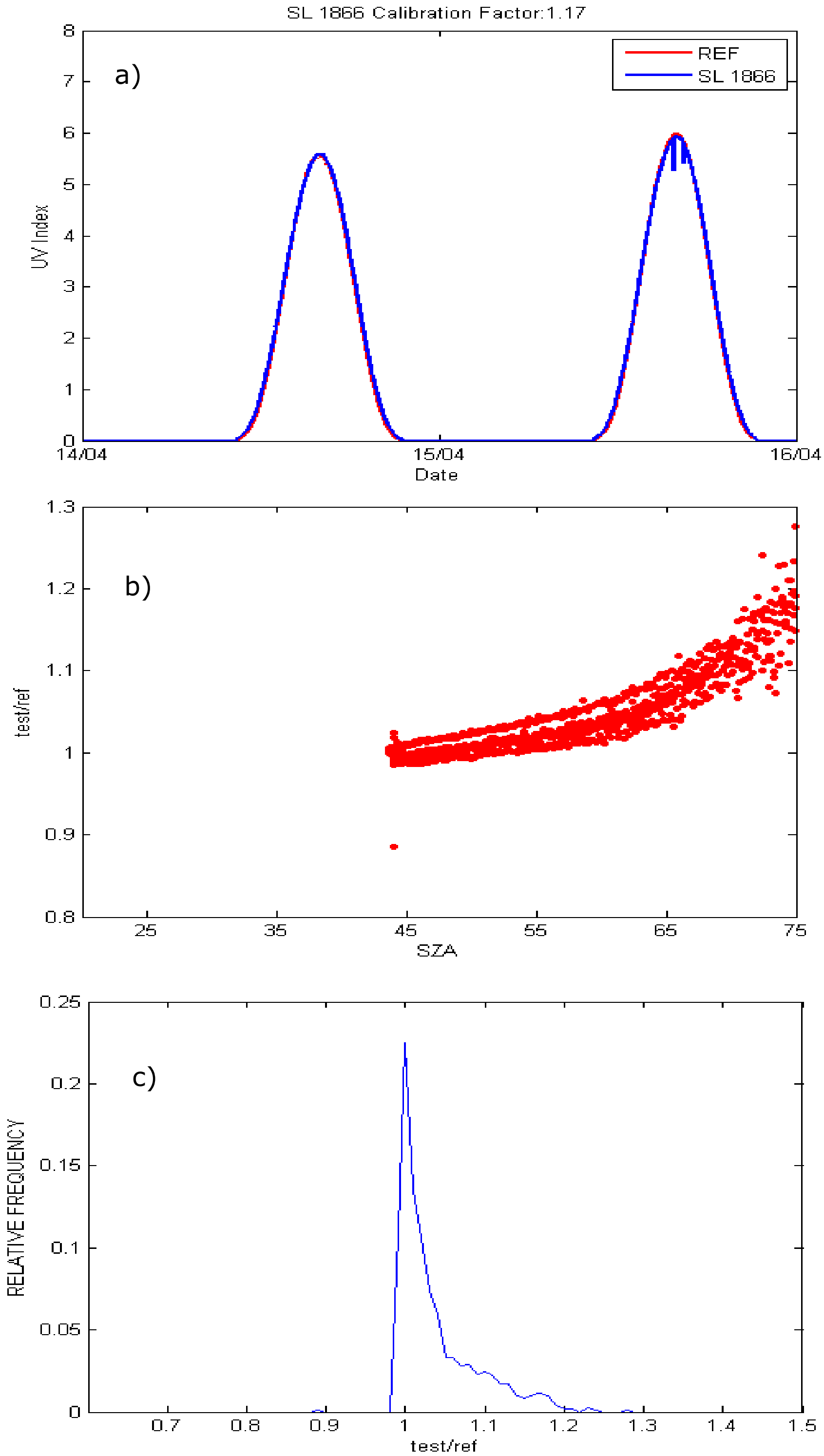

Figure A.1: a) UV index measured by the reference instrument and the SL1866 simultaneously for April 14 and 15. b) Ratio between the corrected values of irradiance for the sensor calibrated (t_{test}) and the values obtained by the reference (t_{ref}). c) Relative frequency of each of the t_{test} / t_{ref} values.

RESULTS OBTAINED FOR SENSOR 1870

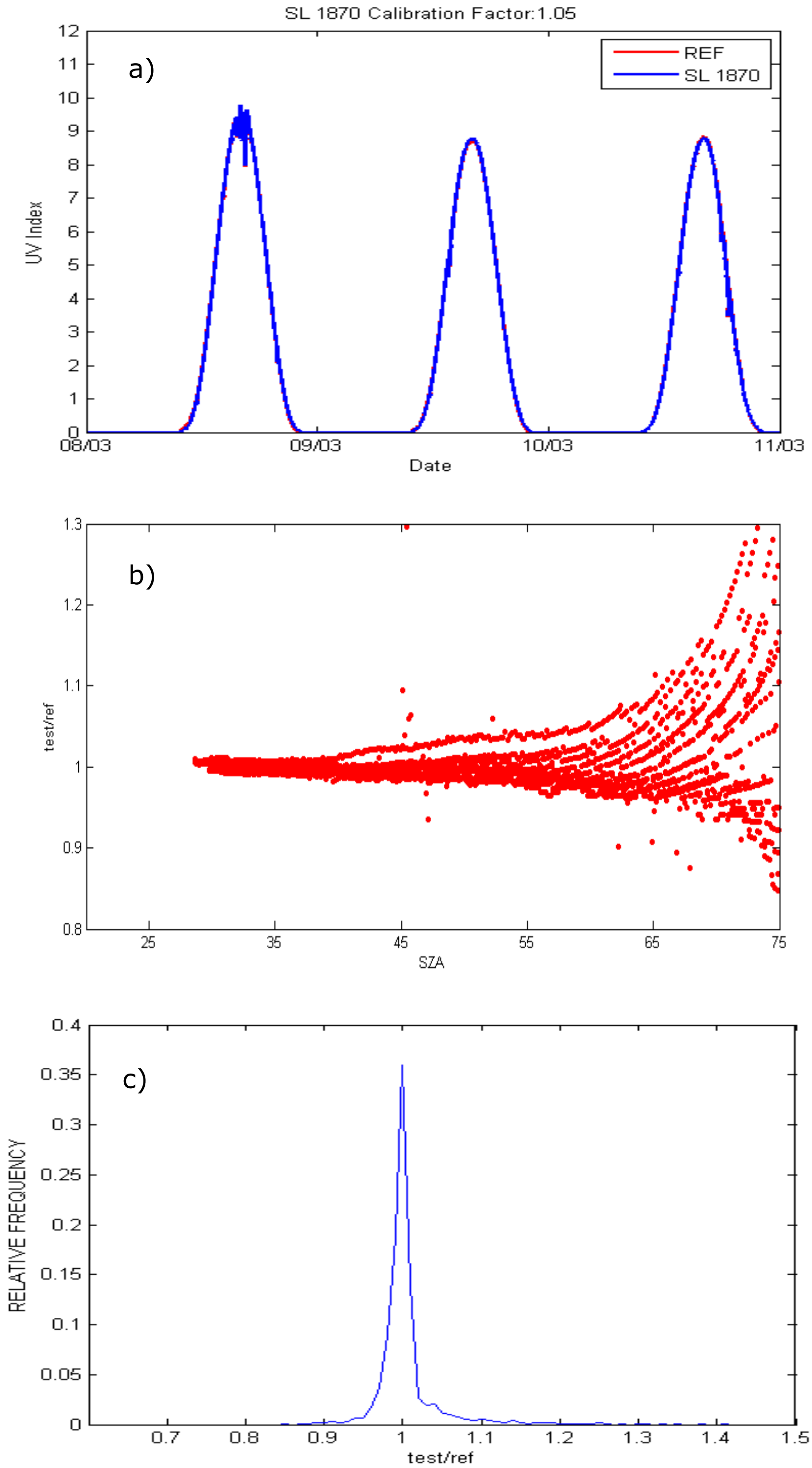

Figure A.2: a) UV index measured by the reference instrument and the SL1870 simultaneously for March 8, 9 and 10. b) Ratio between the corrected values of irradiance for the sensor calibrated (t_{test}) and the values obtained by the reference (t_{ref}). c) Relative frequency of each of the t_{test} / t_{ref} values.

RESULTS OBTAINED FOR SENSOR SL 1871

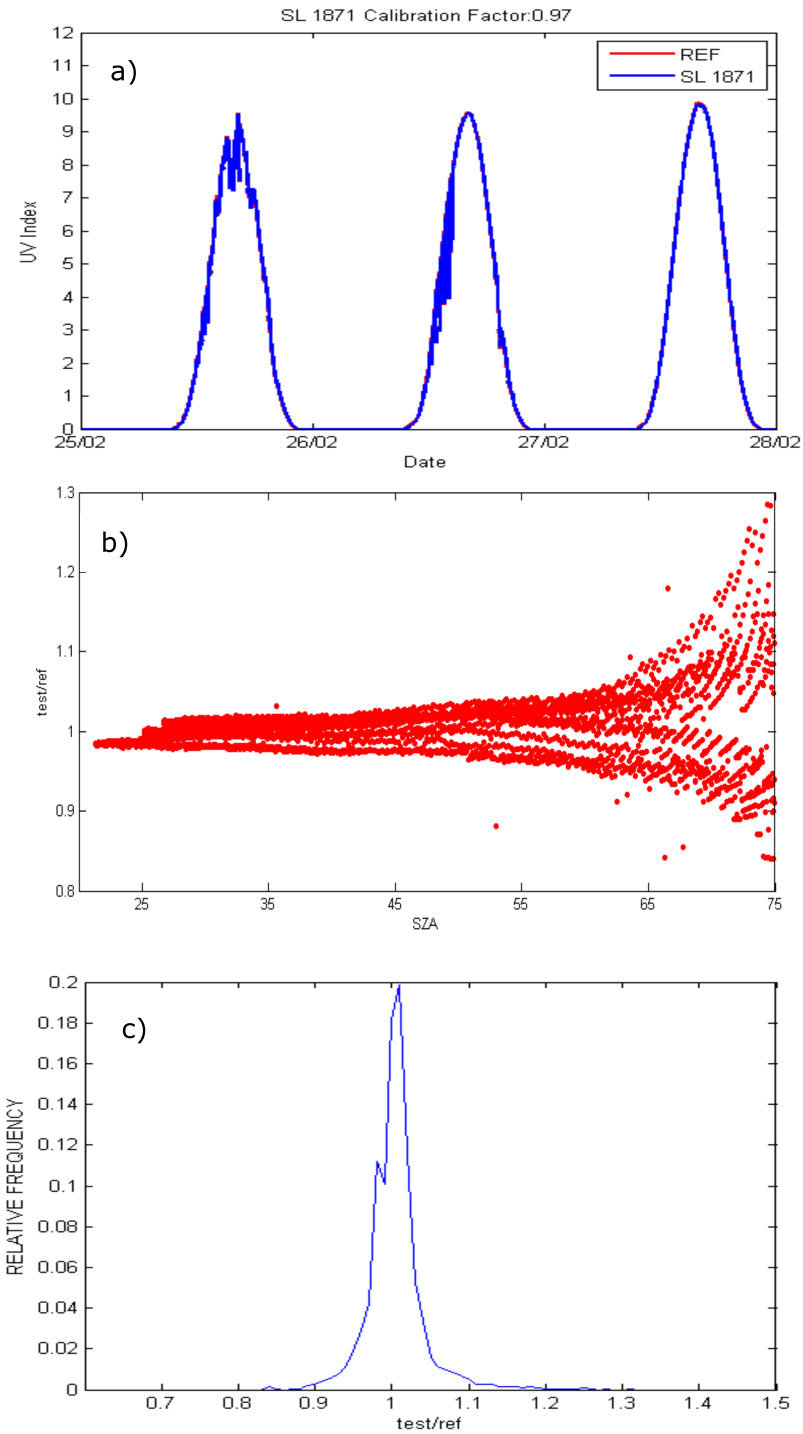

Figure A.3: a) UV index measured by the reference instrument and the SL1871 simultaneously for February 25, 26 and 27. b) Ratio between the corrected values of irradiance for the sensor calibrated (t_{test}) and the values obtained by the reference (t_{ref}). c) Relative frequency of each of the t_{test} / t_{ref} values.

RESULTS OBTAINED FOR SENSOR SL 2711

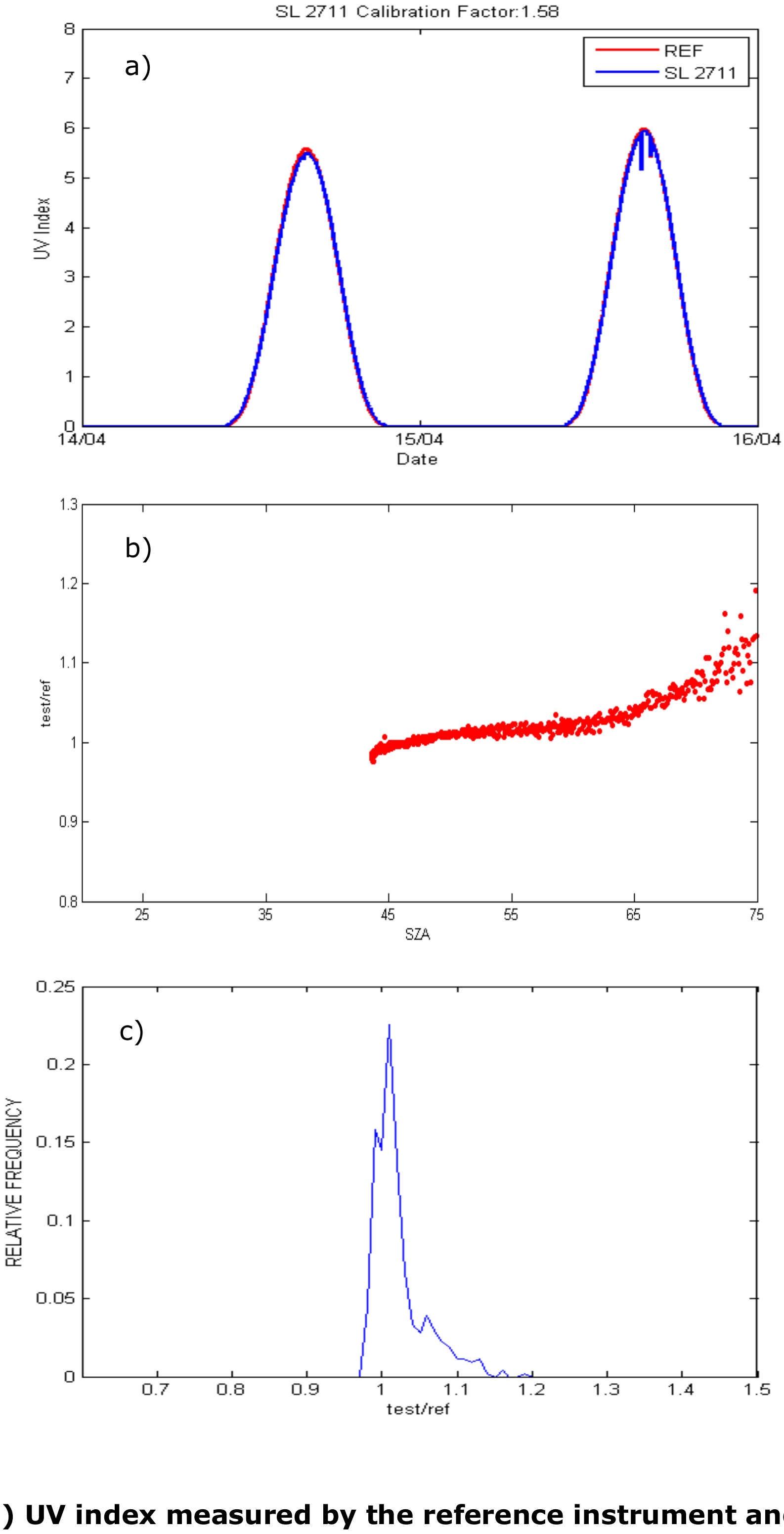

Figure A.4: a) UV index measured by the reference instrument and the SL2711 simultaneously for April 14 and 15. b) Ratio between the corrected values of irradiance for the sensor calibrated (t_{test}) and the values obtained by the reference (t_{ref}). c) Relative frequency of each of the t_{test} / t_{ref} values.

RESULTS OBTAINED FOR SENSOR SL 2747

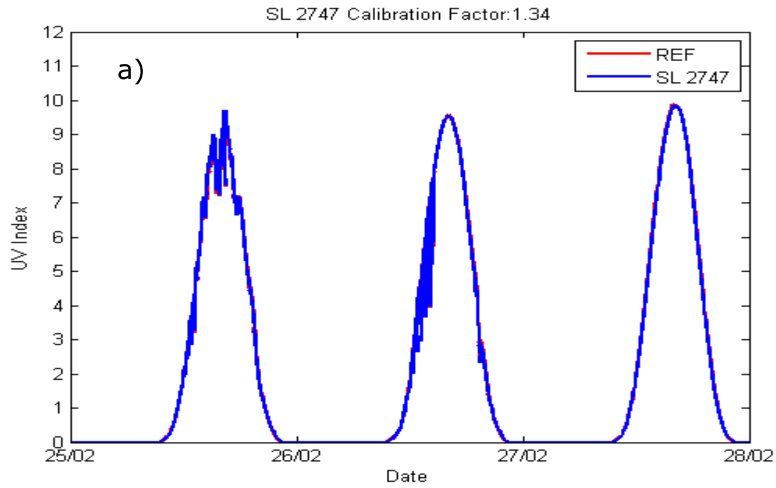

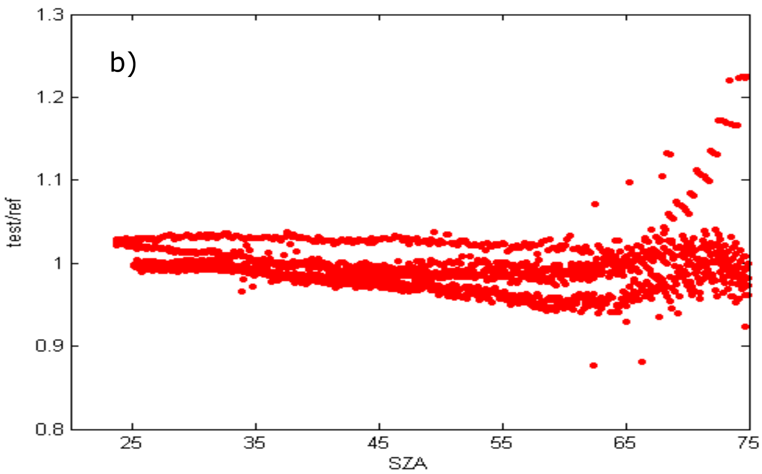

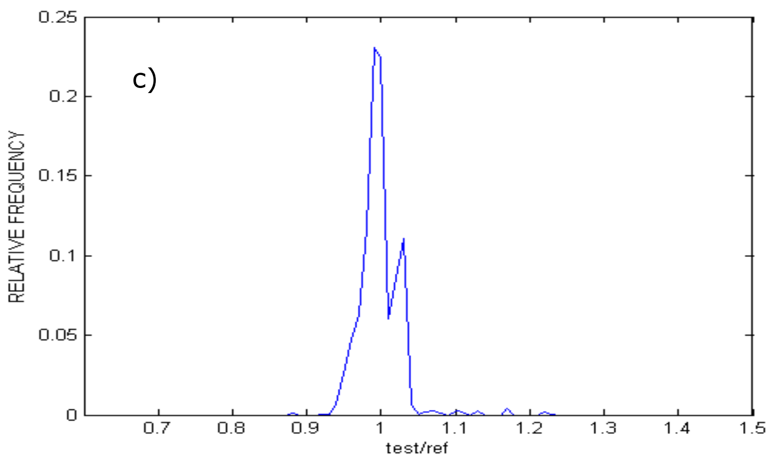

Figure A.5: a) UV index measured by the reference instrument and the SL 2747 simultaneously for February 25, 26 and 27. b) Ratio between the corrected values of irradiance for the sensor calibrated (t_{test}) and the values obtained by the reference (t_{ref}). c) Relative frequency of each of the t_{test} / t_{ref} values.

RESULTS OBTAINED FOR SENSOR SL 2748

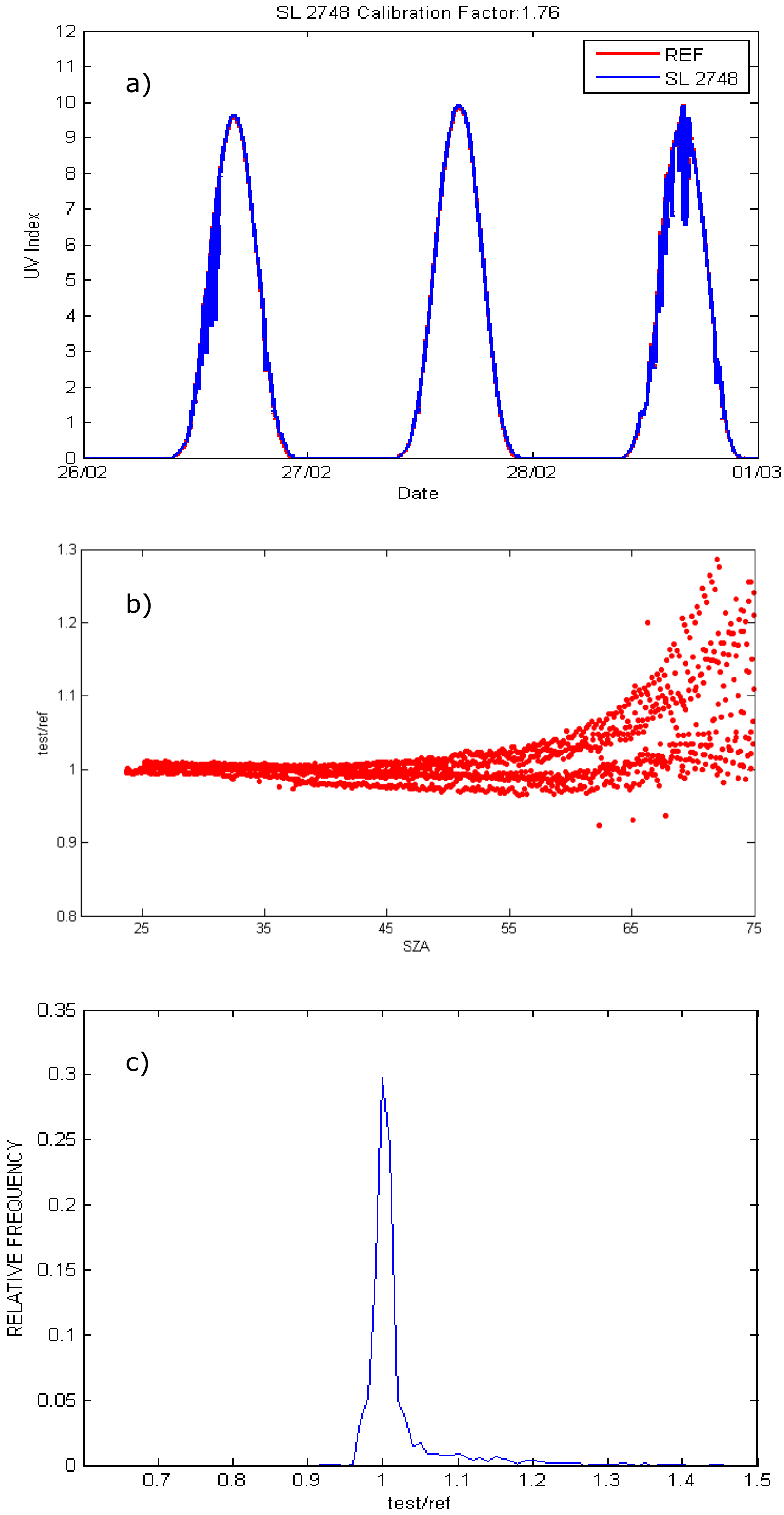

Figure A.6: a) UV index measured by the reference instrument and the SL 2748 simultaneously for February 26, 27 and 28. b) Ratio between the corrected values of irradiance for the sensor calibrated (t_{test}) and the values obtained by the reference (t_{ref}). c) Relative frequency of each of the t_{test} / t_{ref} values.

RESULTS OBTAINED FOR SENSOR SL 2753

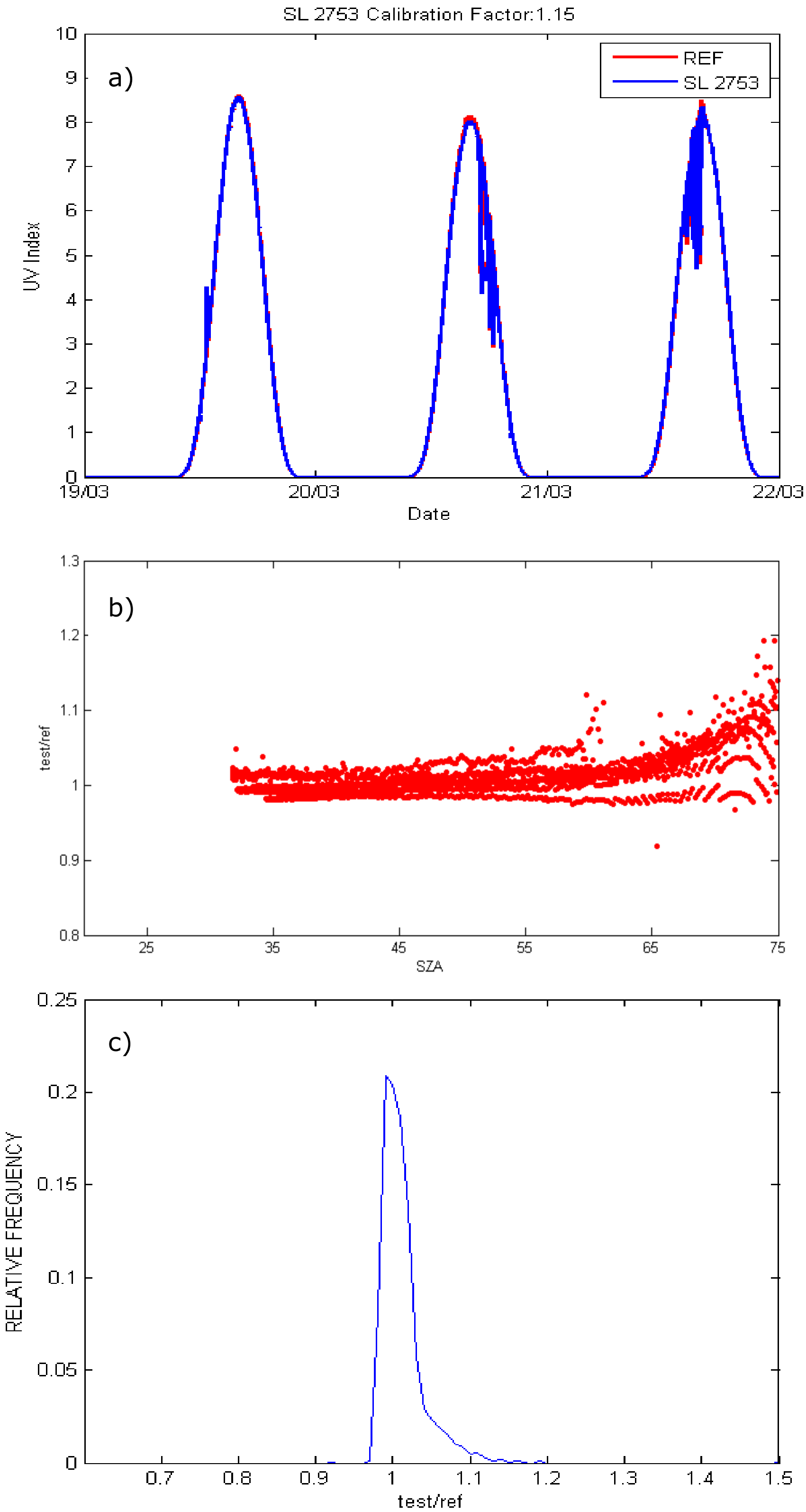

Figure A.7: a) UV index measured by the reference instrument and the SL 2753 simultaneously for March 19, 20 and 21. b) Ratio between the corrected values of irradiance for the sensor calibrated (t_{test}) and the values obtained by the reference (t_{ref}). c) Relative frequency of each of the t_{test} / t_{ref} values.

RESULTS OBTAINED FOR SENSOR SL 9002

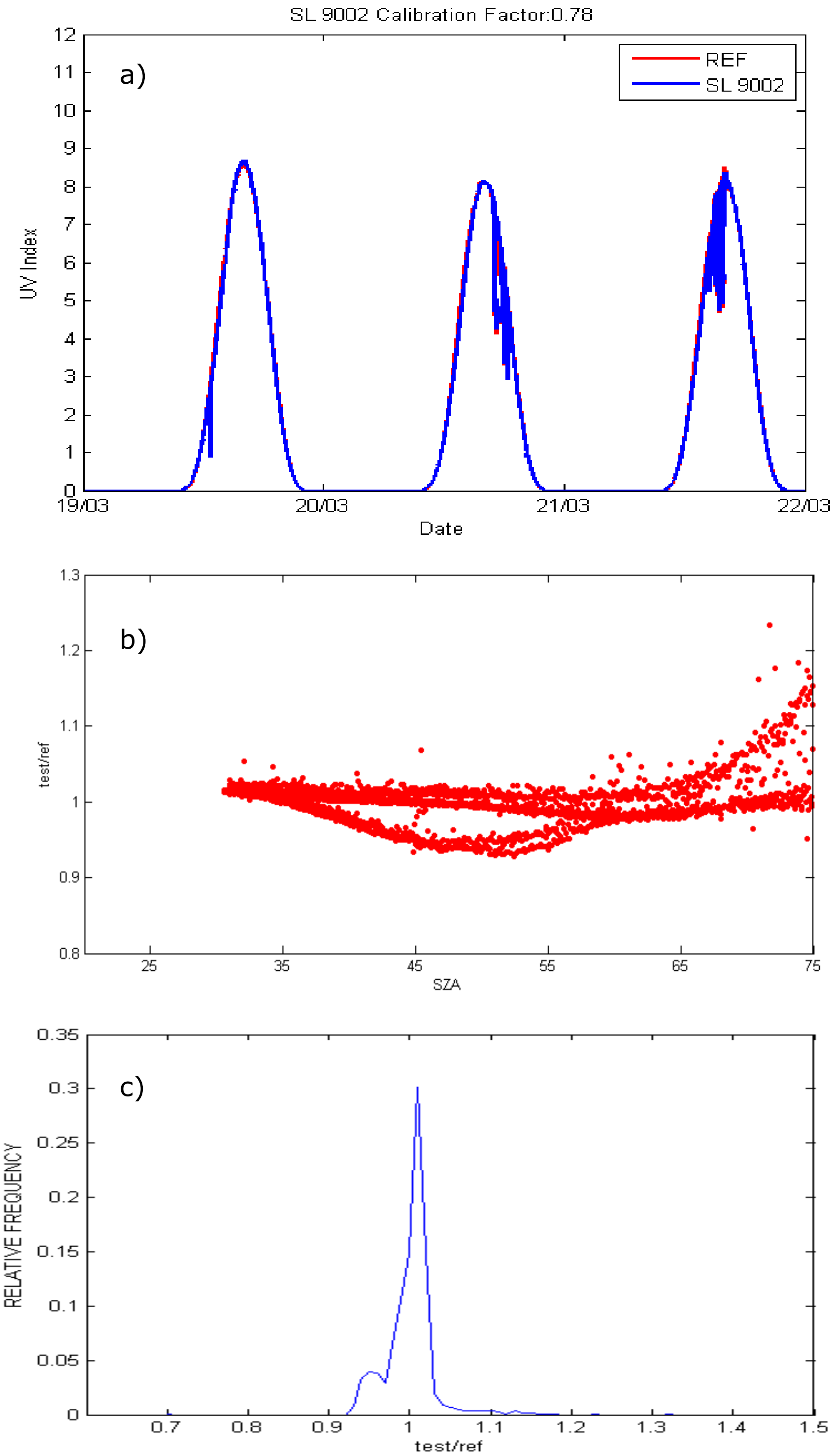

Figure A.8: a) UV index measured by the reference instrument and the SL 9002 simultaneously for March 19, 20 and 21. b) Ratio between the corrected values of irradiance for the sensor calibrated (t_{test}) and the values obtained by the reference (t_{ref}). c) Relative frequency of each of the t_{test} / t_{ref} values.

RESULTS OBTAINED FOR SENSOR SL 9004

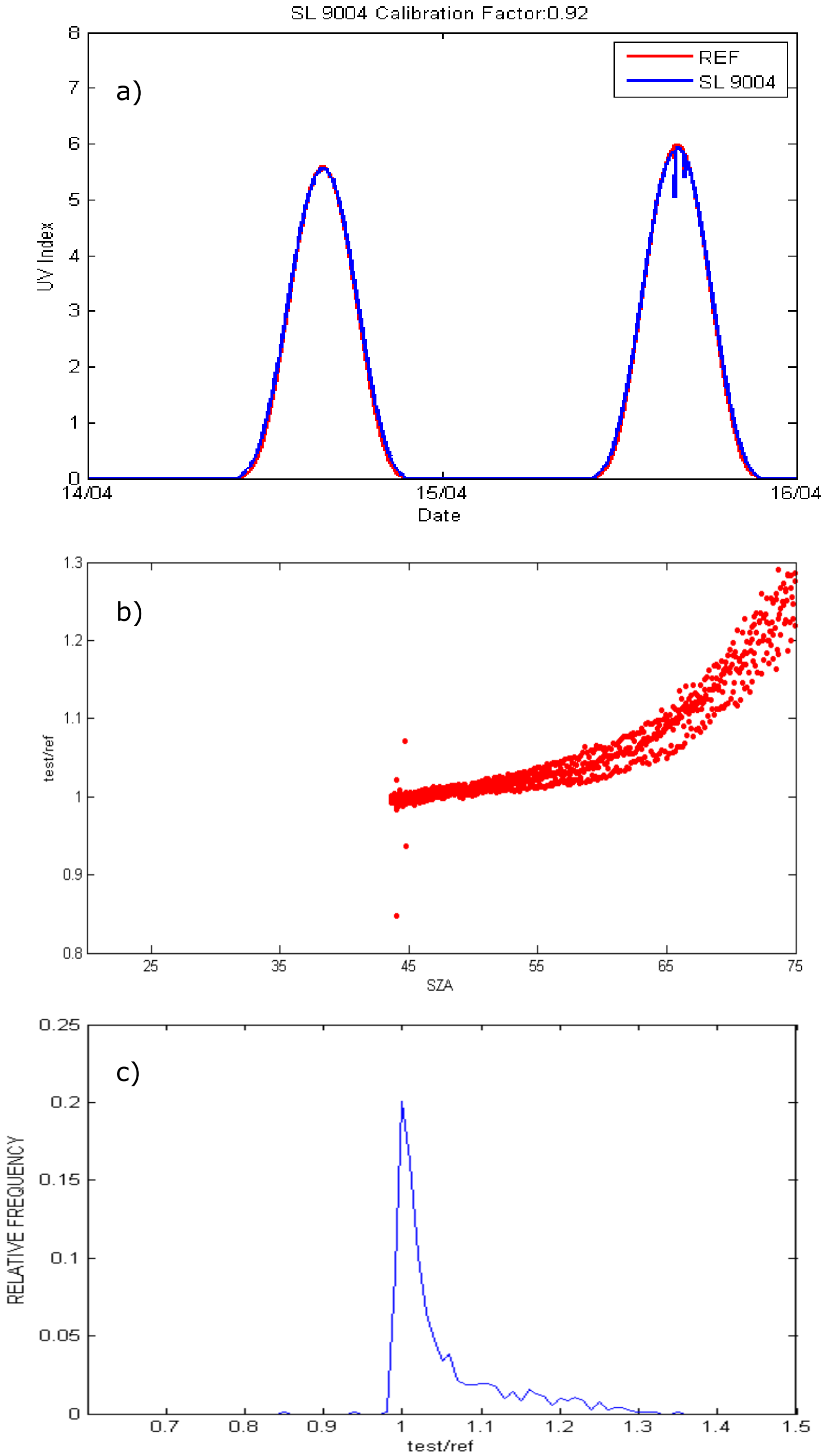

Figure A.9: a) UV index measured by the reference instrument and the SL 9004 simultaneously for April 14 and 15. b) Ratio between the corrected values of irradiance for the sensor calibrated (t_{test}) and the values obtained by the reference (t_{ref}). c) Relative frequency of each of the t_{test} / t_{ref} values.

RESULTS OBTAINED FOR SENSOR YES 60703

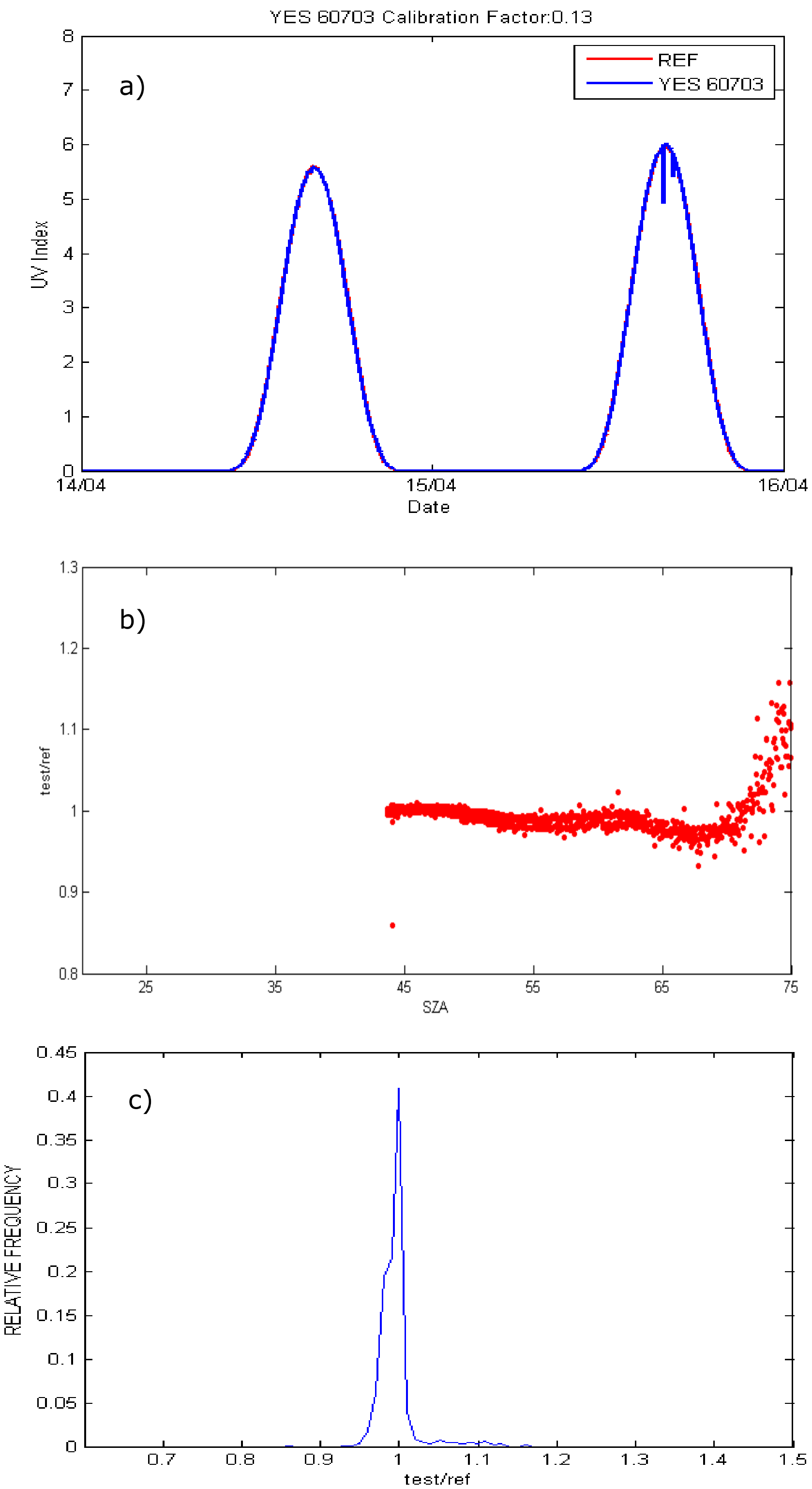

Figure A.10: a) UV index measured by the reference instrument and the YES 60703 simultaneously for April 14 and 15. b) Ratio between the corrected values of irradiance for the sensor calibrated (t_{test}) and the values obtained by the reference (t_{ref}). c) Relative frequency of each of the t_{test} / t_{ref} values.

RESULTS OBTAINED FOR SENSOR YES 130803

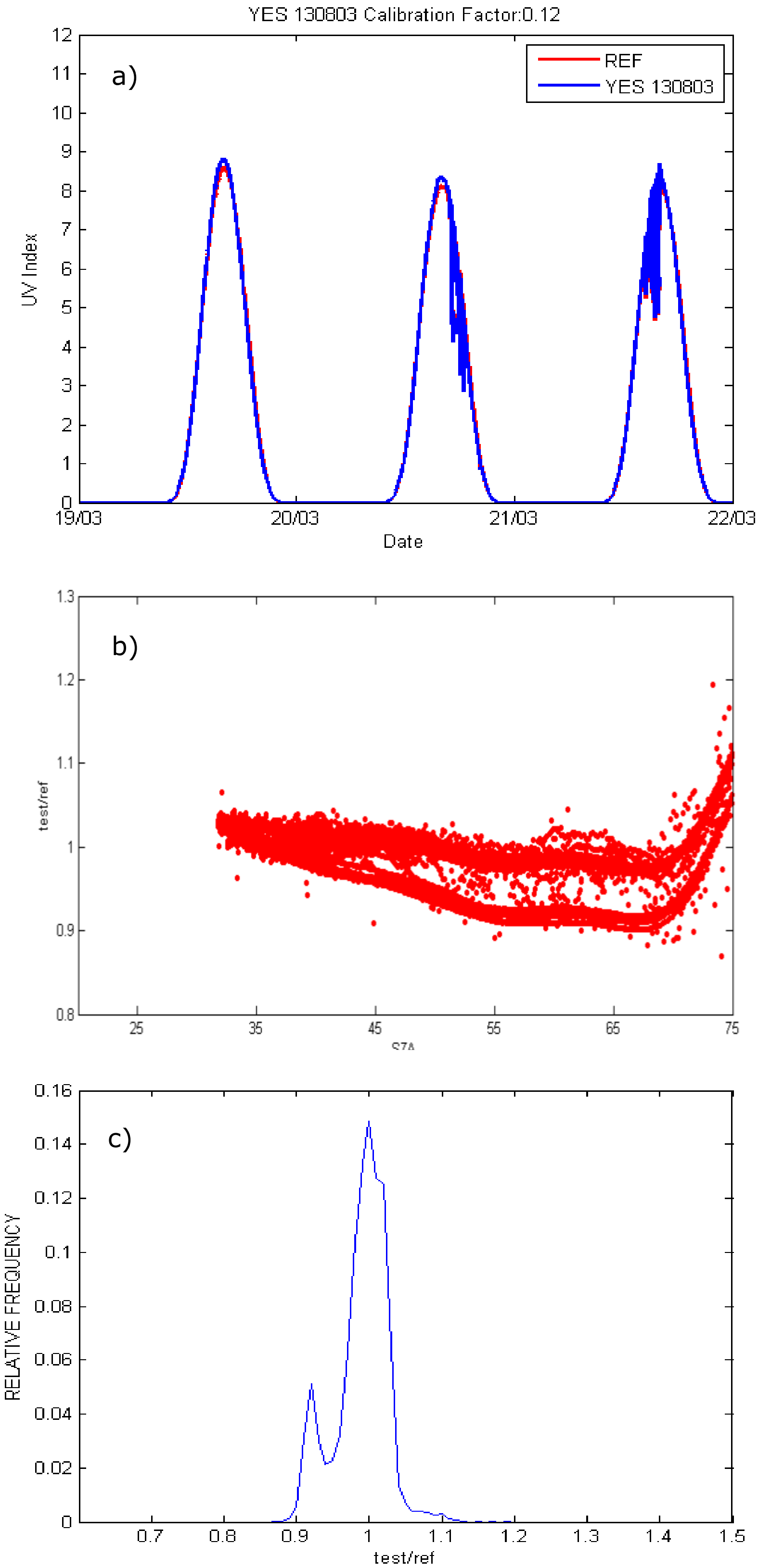

Figure A.11: a) UV index measured by the reference instrument and the YES 130803 simultaneously for March 19, 20 and 21. b) Ratio between the corrected values of irradiance for the sensor calibrated (t_{test}) and the values obtained by the reference (t_{ref}). c) Relative frequency of each of the t_{test} / t_{ref} values.

RESULTS OBTAINED FOR SENSOR YES 130804

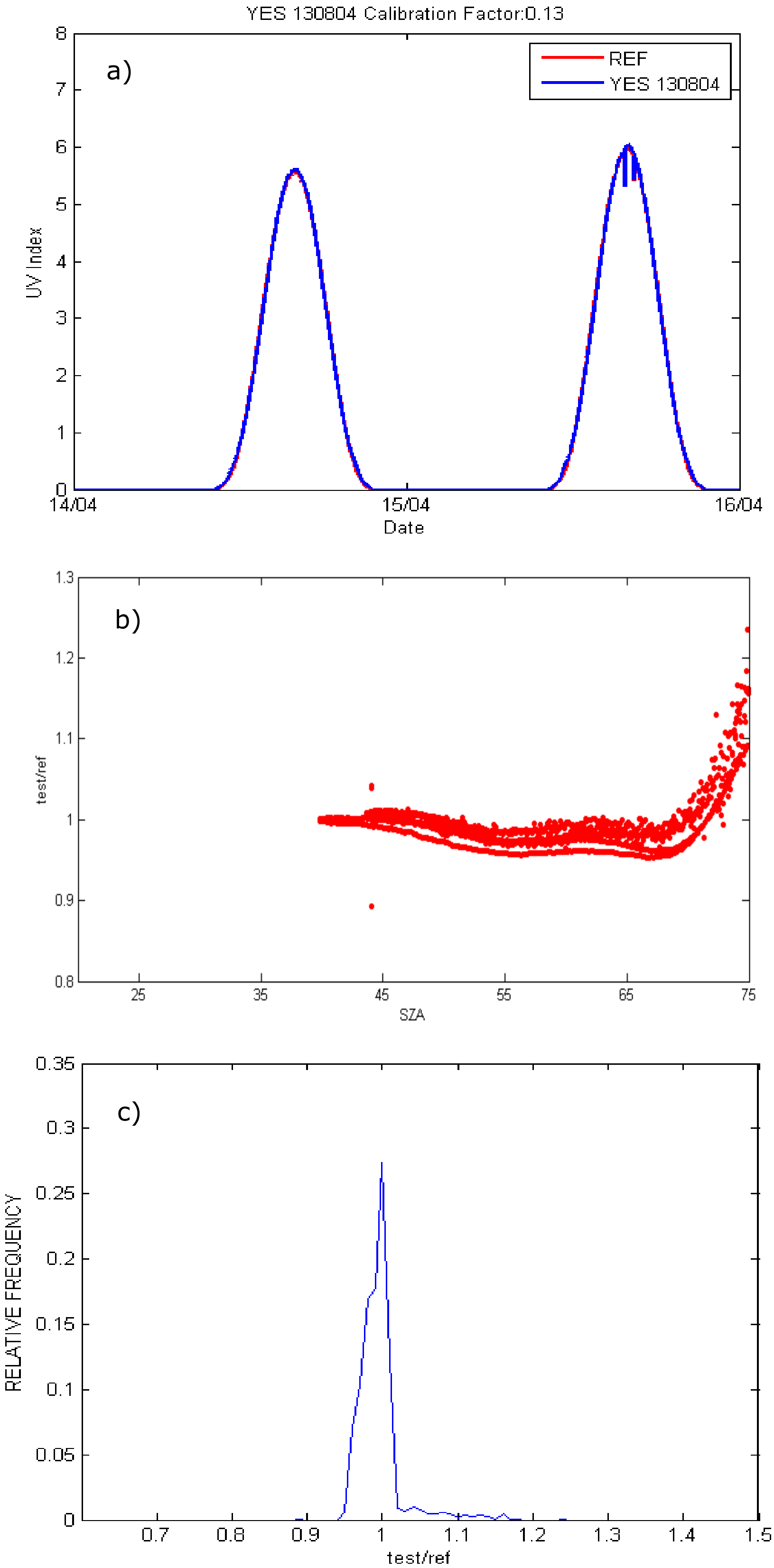

Figure A.12: a) UV index measured by the reference instrument and the YES 130804 simultaneously for April 14 and 15. b) Ratio between the corrected values of irradiance for the sensor calibrated (t_{test}) and the values obtained by the reference (t_{ref}). c) Relative frequency of each of the t_{test} / t_{ref} values.

RESULTS OBTAINED FOR SENSOR YES 130805

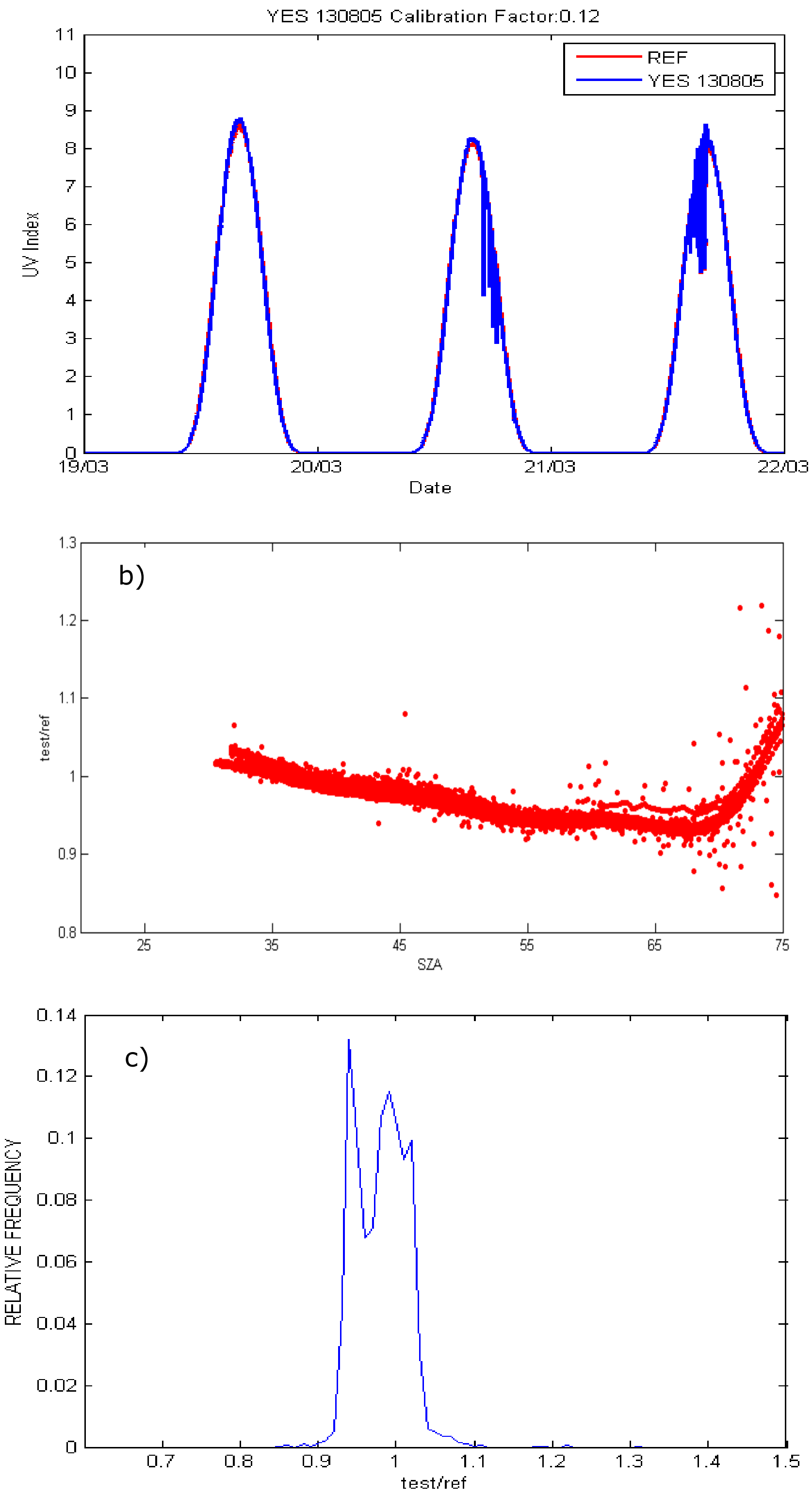

Figure A.13: a) UV index measured by the reference instrument and the YES 130805 simultaneously for March 19, 20 and 21. b) Ratio between the corrected values of irradiance for the sensor calibrated (t_{test}) and the values obtained by the reference (t_{ref}). c) Relative frequency of each of the t_{test} / t_{ref} values.

RESULTS OBTAINED FOR SENSOR YES 130806

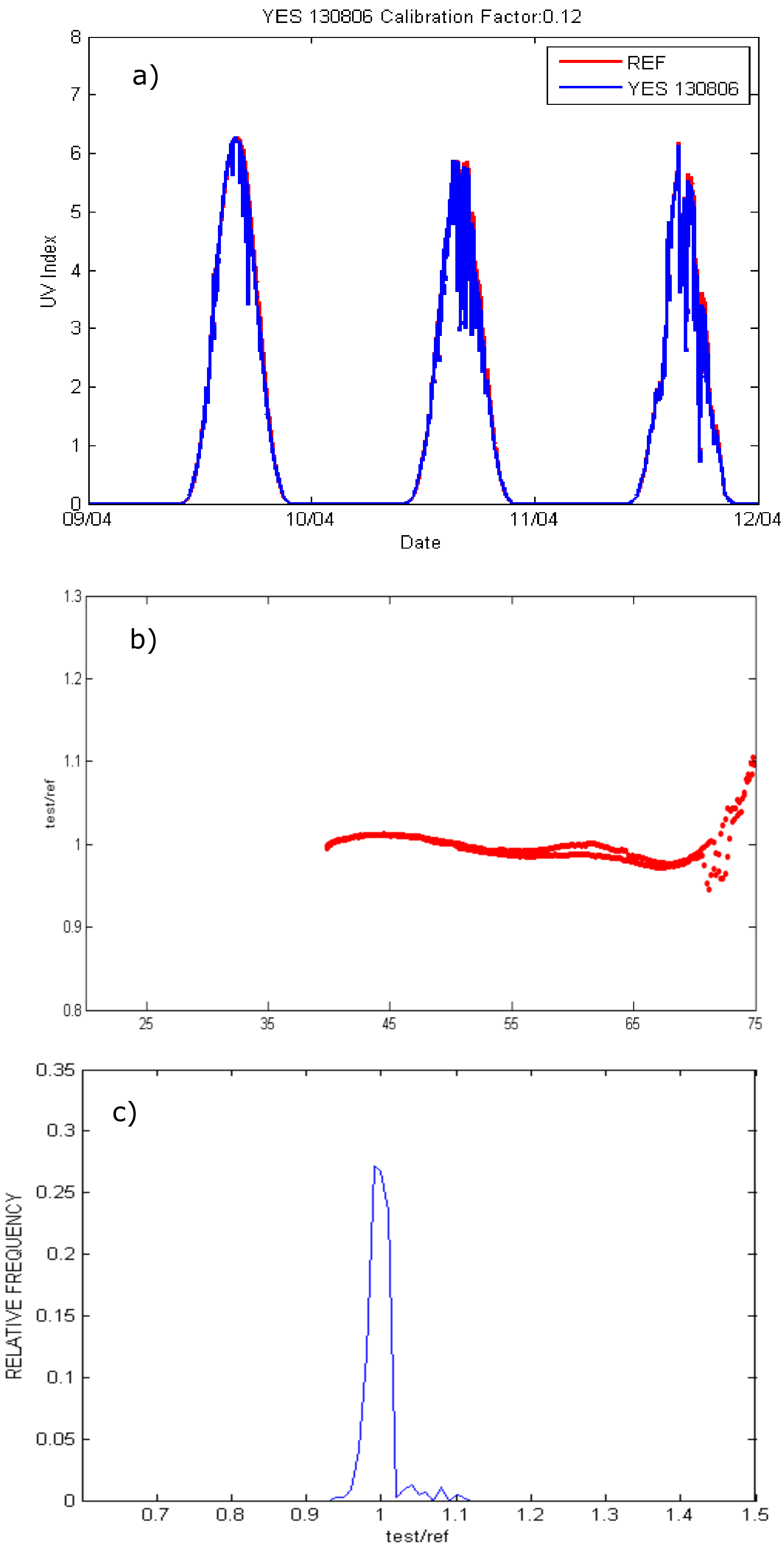

Figure A.14: a) UV index measured by the reference instrument and the YES 130806 simultaneously for April 9, 10 and 11. b) Ratio between the corrected values of irradiance for the sensor calibrated (t_{test}) and the values obtained by the reference (t_{ref}). c) Relative frequency of each of the t_{test} / t_{ref} values.

RESULTS OBTAINED FOR SENSOR YES 940602

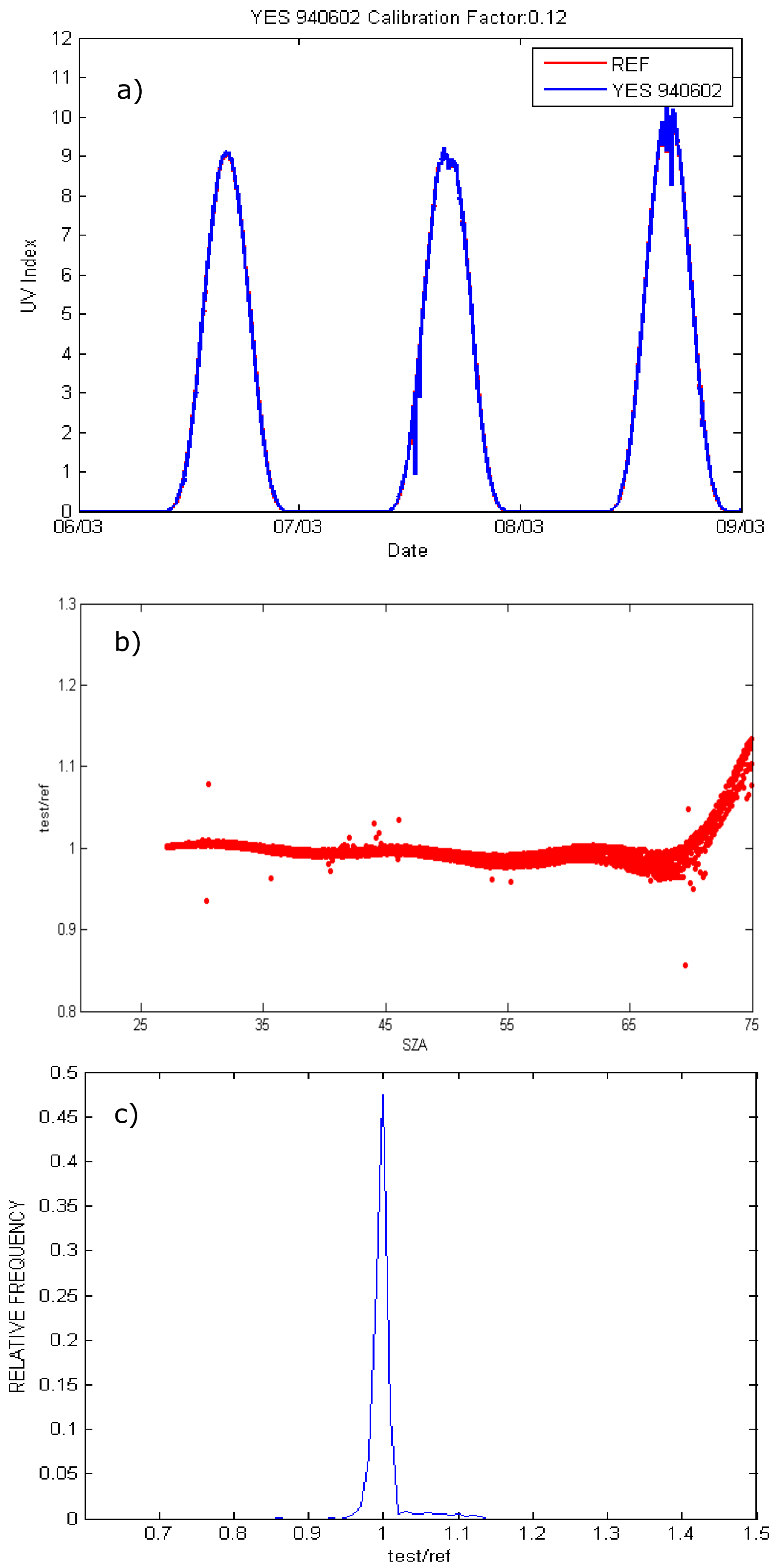

Figure A.15: a) UV index measured by the reference instrument and the YES 940602 simultaneously for March 6,7 and 8. b) Ratio between the corrected values of irradiance for the sensor calibrated (t_{test}) and the values obtained by the reference (t_{ref}). c) Relative frequency of each of the t_{test} / t_{ref} values.

RESULTS OBTAINED FOR SENSOR YES 970809

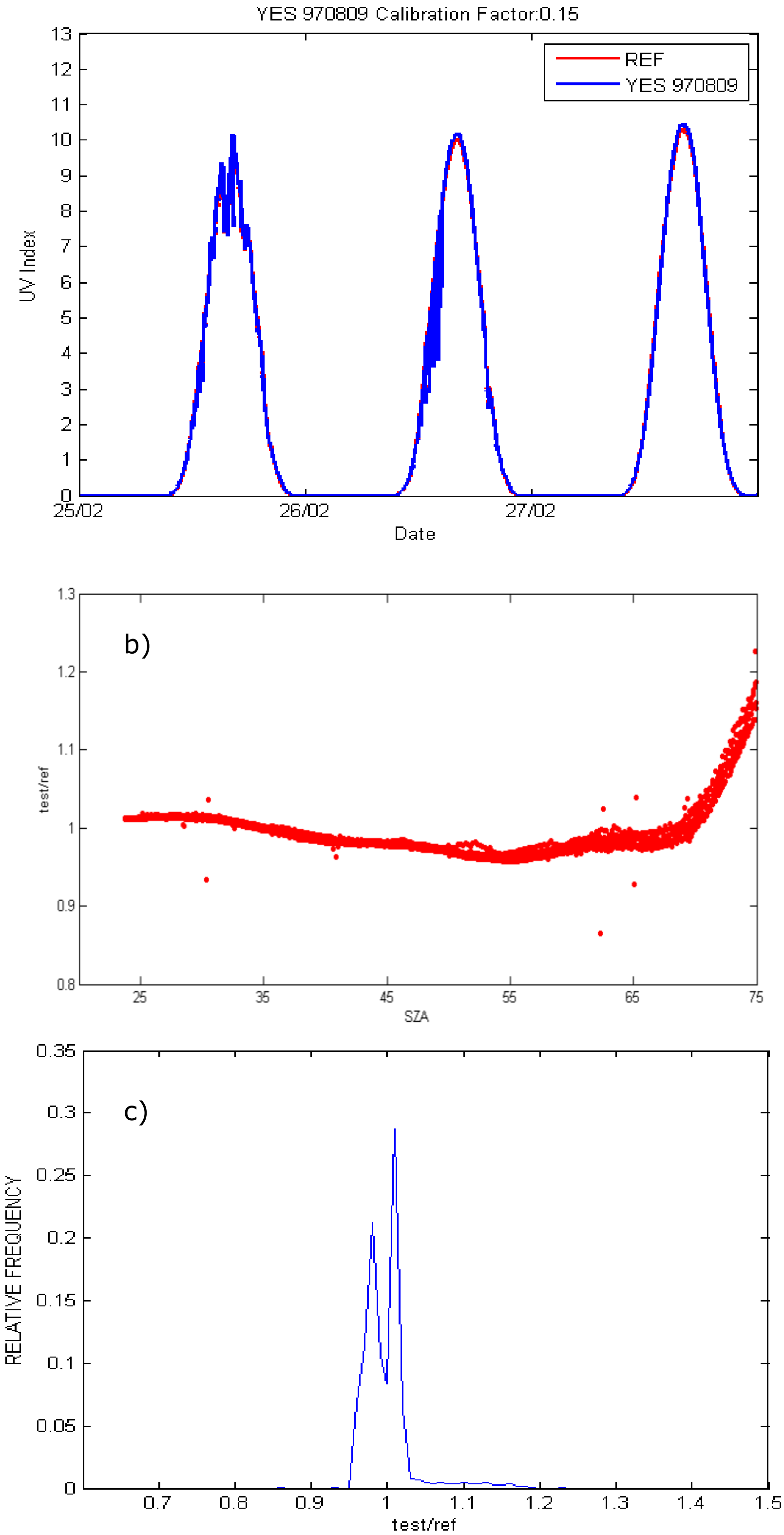

Figure A.16: a) UV index measured by the reference instrument and the YES 970809 simultaneously for February 25, 26 and 27. b) Ratio between the corrected values of irradiance for the sensor calibrated (t_{test}) and the values obtained by the reference (t_{ref}). c) Relative frequency of each of the t_{test} / t_{ref} values.

RESULTS OBTAINED FOR SENSOR YES 970811

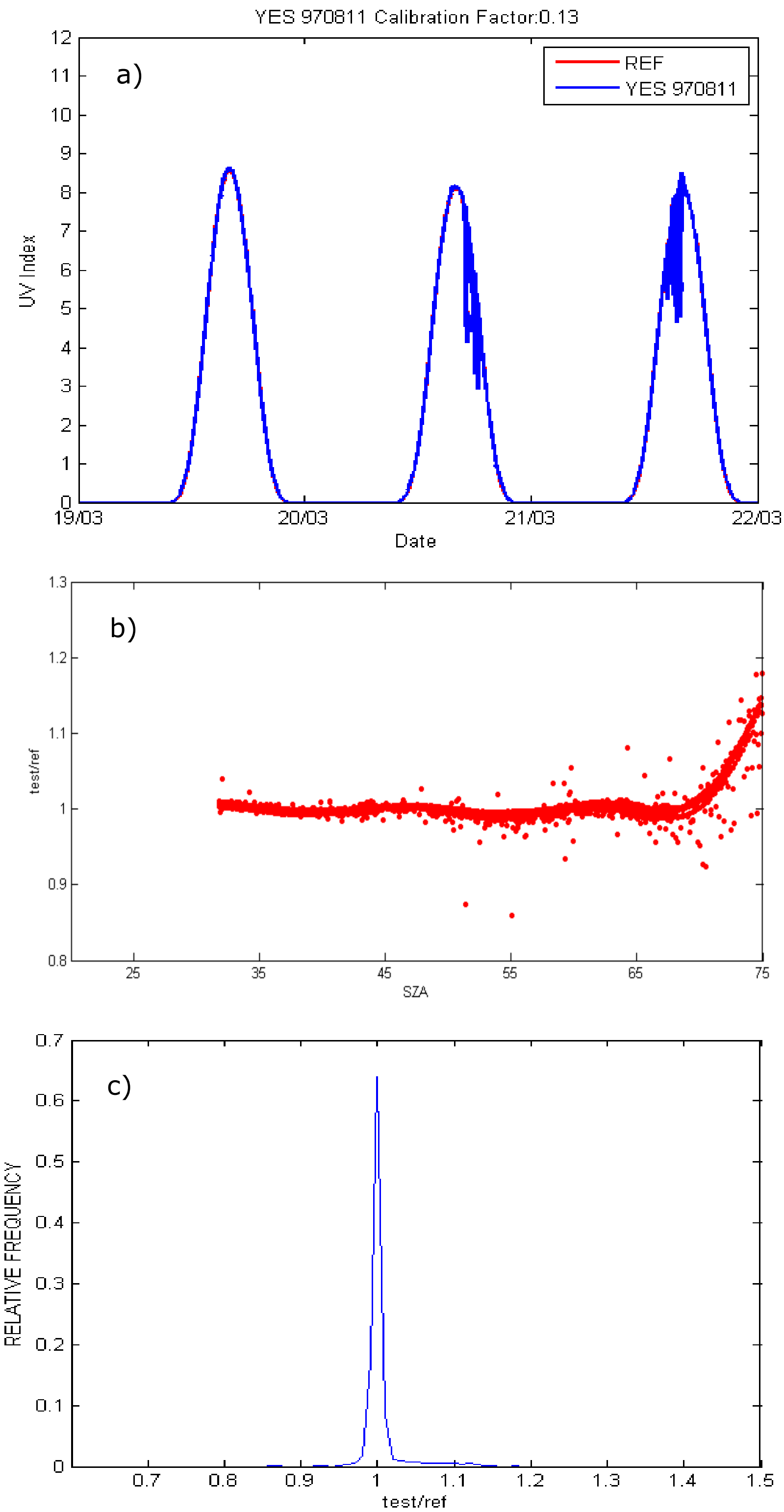

Figure A.17: a) UV index measured by the reference instrument and the YES 970811 simultaneously for March 19, 20 and 21. b) Ratio between the corrected values of irradiance for the sensor calibrated (t_{test}) and the values obtained by the reference (t_{ref}). c) Relative frequency of each of the t_{test} / t_{ref} values.

RESULTS OBTAINED FOR SENSOR K&Z 120059

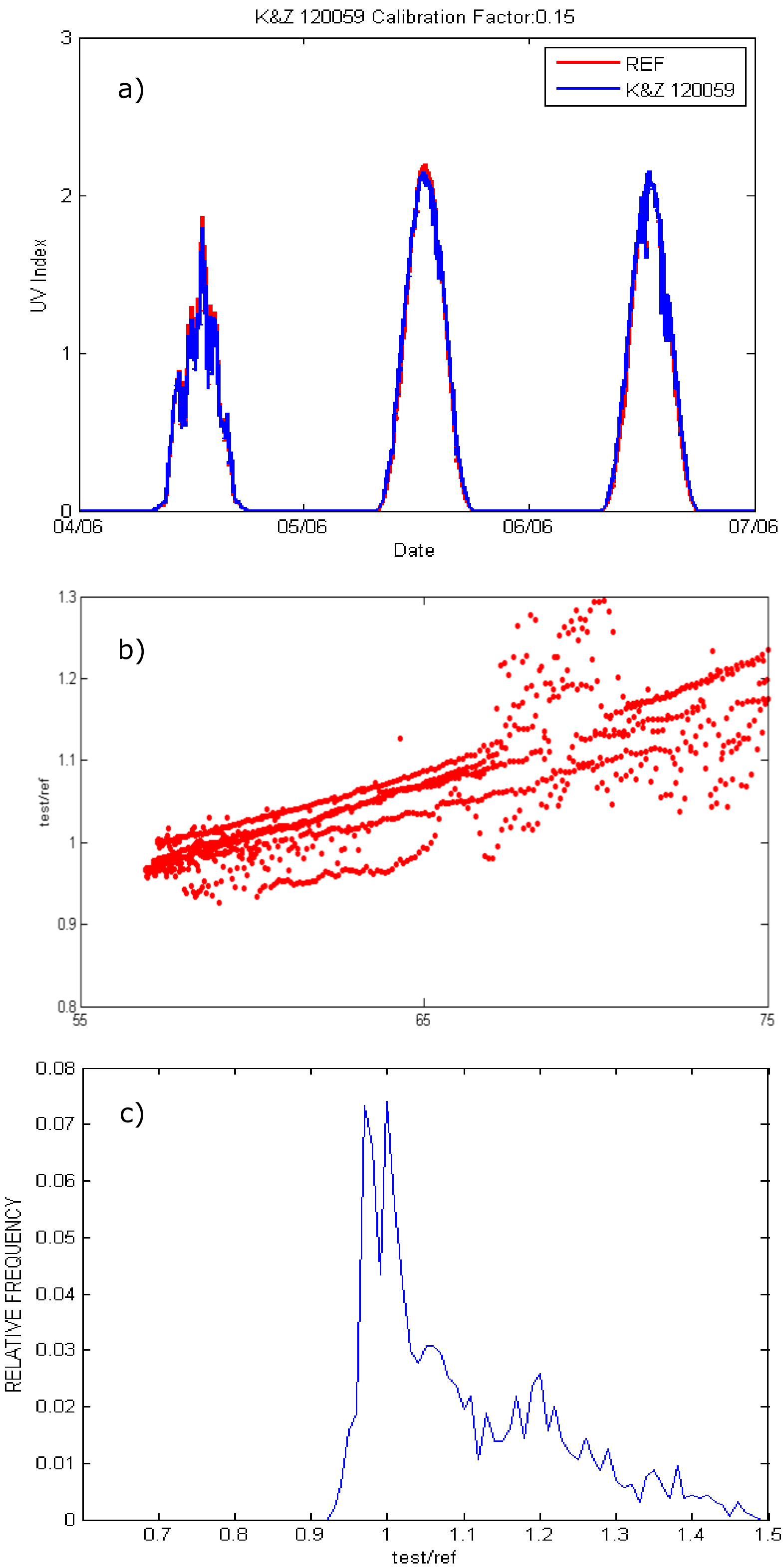

Figure A.18: a) UV index measured by the reference instrument and the K&Z 120059 simultaneously for June4, 5 and 6. b) Ratio between the corrected values of irradiance for the sensor calibrated (t_{test}) and the values obtained by the reference (t_{ref}). c) Relative frequency of each of the t_{test} / t_{ref} values.

RESULTS OBTAINED FOR SENSOR K&Z 170212

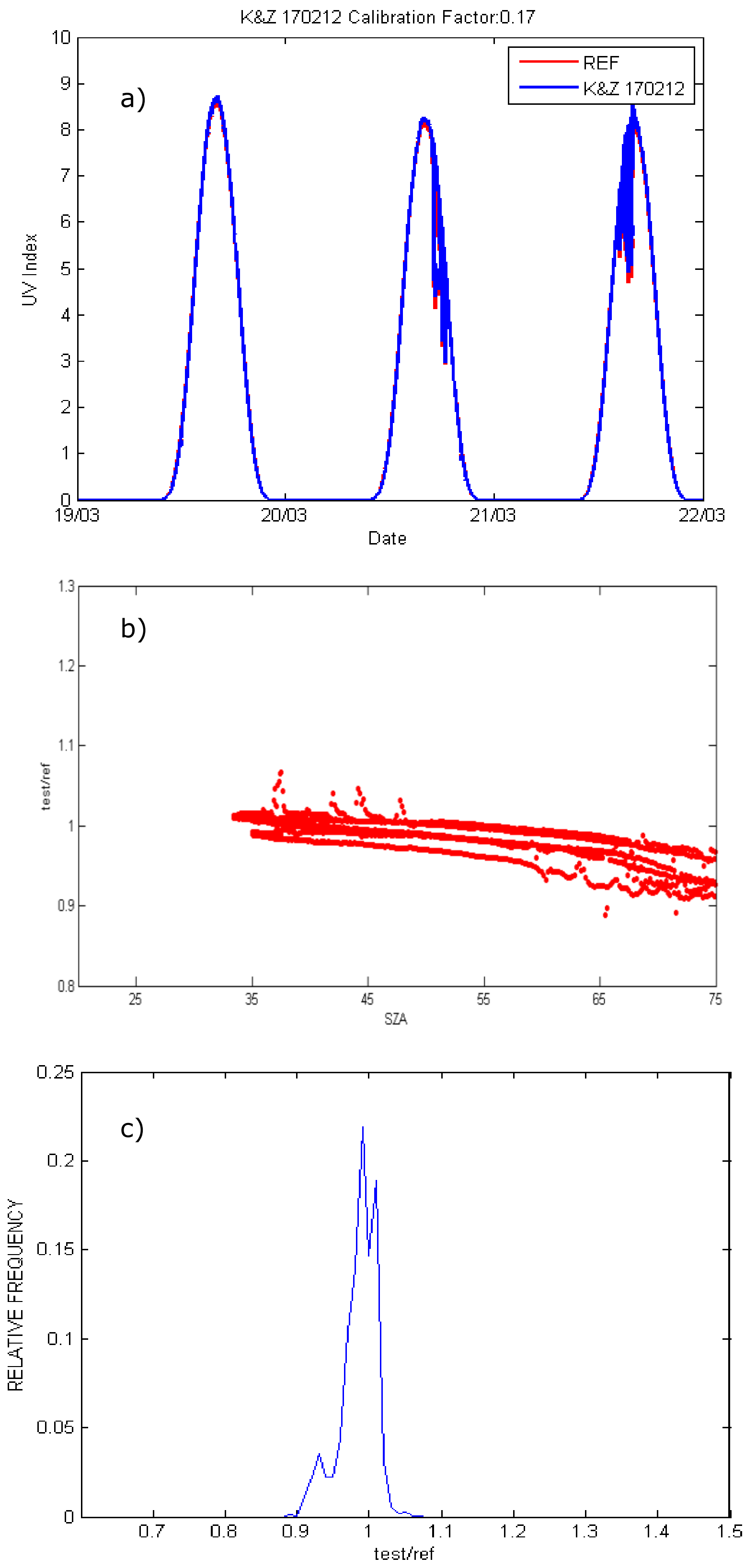

Figure A.19: a) UV index measured by the reference instrument and the K&Z 170212 simultaneously for March 19, 20 and 21. b) Ratio between the corrected values of irradiance for the sensor calibrated (t_{test}) and the values obtained by the reference (t_{ref}). c) Relative frequency of each of the t_{test} / t_{ref} values.

RESULTS OBTAINED FOR SENSOR K&Z 170213

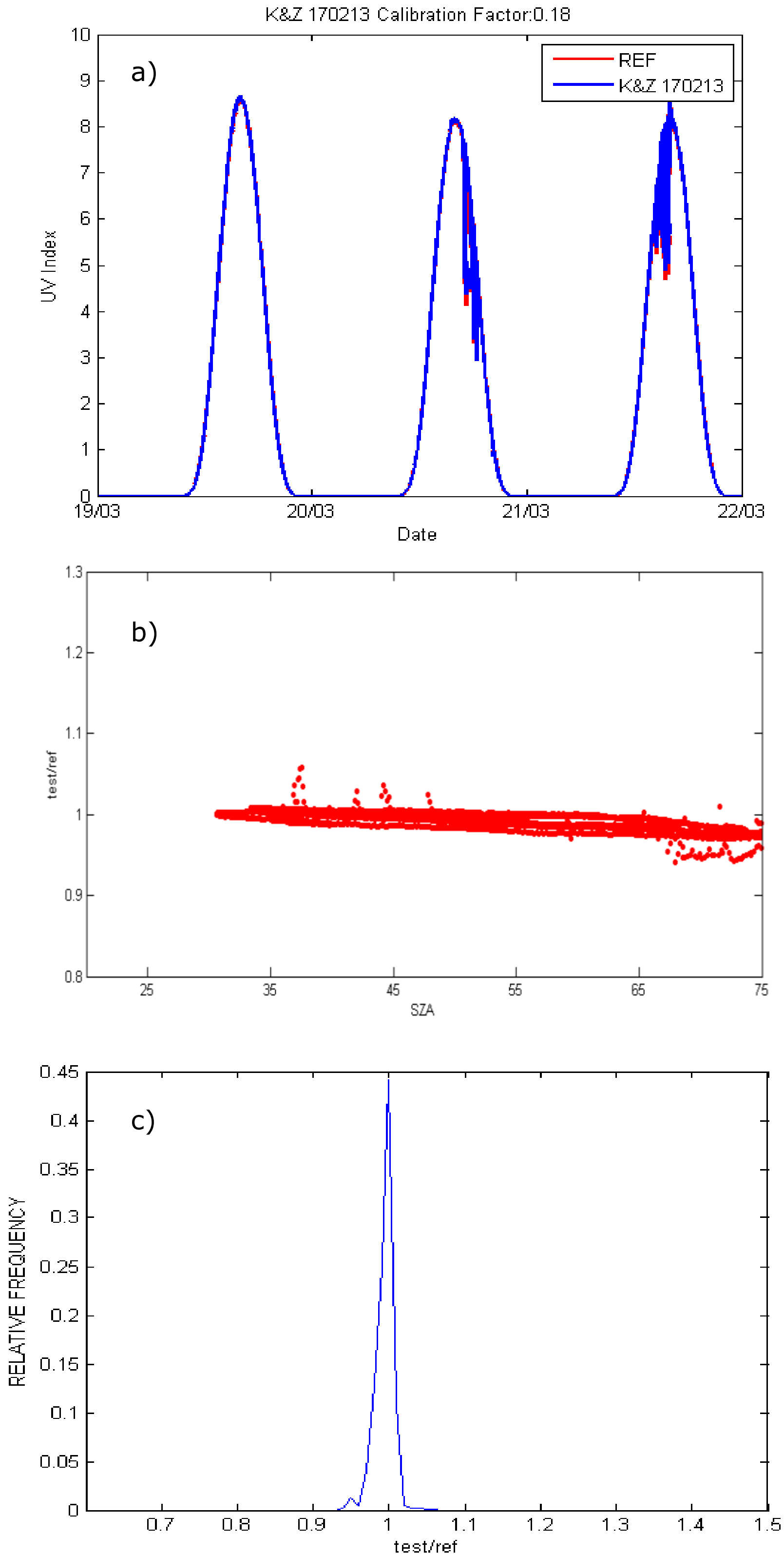

Figure A.20: a) UV index measured by the reference instrument and the K&Z 170213 simultaneously for March 19, 20 and 21. b) Ratio between the corrected values of irradiance for the sensor calibrated (t_{test}) and the values obtained by the reference (t_{ref}). c) Relative frequency of each of the t_{test} / t_{ref} values.

LIST OF RECENT GAW REPORTS*

242. 19th WMO/IAEA Meeting on Carbon Dioxide, Other Greenhouse Gases and Related Tracers Measurement Techniques (GGMT-2017), Dübendorf, Switzerland, 27-31 August 2017, 2018.

241. SPARC/IOC/GAW Report on Long-term Ozone Trends and Uncertainties in the Stratsophere, SPARC Report No. 9, WCRP-2017/2018, GAW Report No. 241, 2018.

240. Report of the Second International UV Filter Radiometer Intercomparison UVC-II, Davos, Switzerland, 25 May-5 October 2017, 212 pp., 2018.

239. Calibration Methods of GC-μECD for Atmospheric SF6 Measurements, 26 pp., 2018.

238. The Magnitude and Impacts of Anthropogenic Atmospheric Nitrogen Inputs to the Ocean, Reports and Studies GESAMP No. 97, 47 pp., 2018.

237. Final Report of the 44th Session of GESAMP, Geneva, Switzerland, 4-7 September 2017, Reports and Studies GESAMP No. 96, 115 pp., 2018.

236. Izaña Atmospheric Research Center: Activity Report 2015-2016, 178 pp., 2017.

235. Vegetation Fire and Smoke Pollution Warning and Advisory System (VFSP-WAS): Concept Node and Expert Recommendations, 45 pp., 2018.

234. Global Atmosphere Watch Workshop on Measurement-Model Fusion for the Global Total Atmospheric Deposition (MMF-GTAD), Geneva, Switzerland, 28 February to 2 March 2017, 45 pp., 2017.

233. Report of the Third Session of the CAS Environmental Pollution and Atmospheric Chemistry Scientific Steering Committee (EPAC SSC), Geneva, Switzerland, 15-17 March 2016, 44 pp., 2018.

232. Report of the WMO/GAW Expert Meeting on Nitrogen Oxides and International Workshop on the Nitrogen Cycle, York, UK, 12-14 April 2016, 62 pp., 2017.

231. The Fourth WMO Filter Radiometer Comparison (FRC-IV), Davos, Switzerland, 28 September–16 October 2015, 65 pp., November 2016.

230. Airborne Dust: From R&D to Operational Forecast 2013-2015 Activity Report of the SDS-WAS Regional Center for Northern Africa, Middle East and Europe, 73 pp., 2016.

229. 18th WMO/IAEA Meeting on Carbon Dioxide, Other Greenhouse Gases and Related Tracers Measurement Techniques (GGMT-2015), La Jolla, CA, USA, 13-17 September 2015, 150 pp., 2016.

228. WMO Global Atmosphere Watch (GAW) Implementation Plan: 2016-2023, 81 pp., 2017.

A full list is available at:
http://www.wmo.int/pages/prog/arep/gaw/gaw-reports.html
http://library.wmo.int/opac/index.php?lvl=etagere_see&id=144#.WK2TTBiZNB

For more information, please contact:

World Meteorological Organization

Research Department

Atmospheric Research and Environment Branch

7 bis, avenue de la Paix – P.O. Box 2300 – CH 1211 Geneva 2 – Switzerland

Tel.: +41 (0) 22 730 81 11 – Fax: +41 (0) 22 730 81 81

Email: GAW@wmo.int

Website: http://www.wmo.int/pages/prog/arep/gaw/gaw_home_en.html

JN 181941